Thermal Effects in the Atmospheric Boundary Layer above the North Sea

by

Saskia Tautz

A thesis submitted in partial fulfillment of the requirements for the degree of Diplom in Physics. Presented to the Faculty of Mathematics and Science of the Carl von Ossietzky University of Oldenburg.

Surveyors:

Prof. Dr. Jürgen Parisi
Dr. Detlev Heinemann

Oldenburg, September 2004

Contents

Chapter 1

Introduction

Accurate flux measurements play a decisive role in the atmospheric sciences, for example in climate modelling, weather models and air-sea interaction. They reveal the wind profile and it's dependencies on temperature and surface roughness, setting the boundary conditions for processes in the atmospheric boundary layer.

It seemed that a solid way of describing the lower atmosphere had been found, when Obukhov discovered a universal length scale for exchange processes in the surface layer, which lead to the Monin-Obukhov similarity theory. One of the experimental fundaments of this modern boundary layer physics, was the KANSAS experiment, from which Businger et al. (1971) developed universal functions describing flux-profile relations.
Certain developments lead to doubts in the overall validity of the Monin-Obukhov similarity theory: On the one hand, findings were made, which didn't fit into the theory and on the other hand, a great progress was made in measurement techniques, correction methods and instrumental development. Additionally the whole theory had been developed for dry air and the universal functions were derived for dry air as well. A transfer to situations where the air moisture is much higher (e.g. offshore sites) can be problematic.
A comprehensive and more detailed overview of the history of this part of boundary layer physics has been given by Foken (2004).
Most of the measurement problems that for example occurred at the KANSAS experiment can be minimized with the progress anemometer development has made in the last years. Not only the accuracy of the anemometers themselves, but also correction methods for misalignment, flow distortion of the instrument and mast shadowing have been developed and improved over the course of 20 years.
Also measurement sites are now positioned at a great range of surroundings, including heights of nearly 100m, contrary to the measurement height of about 10m from the ground used in early experiments, and additionally at offshore locations,

for measurements in moist air.
Concluding, new measurements in the atmospheric boundary layer would be a good starting point to investigate atmospheric physics and the validity of Monin-Obukhov as well as maybe finding a more general theory.

In this work, the foundation stone for such a measurement is laid.
At the FINO measurement platform 40km north of Borkum, three ultra-sonic anemometers and other meteorological measurement instruments are employed at a measurement mast of 100m height. The ultrasonic anemometers are positioned at heights of 40m, 60m and 80m, allowing to investigate the wind and flux profiles of the measurement site.
Prior to installation, the calibration of the ultrasonic anemometers was tested in the Oldenburg wind tunnel. It was found that the calibration was partly erroneous and incomplete. A three dimensional calibration method has been developed that takes in account the dependency of the flow distortion for azimuth and elevation angle, as well as for the wind speed. Certain symmetries and linearities of this dependencies could be utilised.
After applying this correction and validating the measurements from FINO, heat and momentum fluxes were calculated. The first flux measurements of the offshore site are presented and the influence of the enhanced calibration is investigated. Also, some initial analysis has been conducted.

In chapter two, a short summary of the basic principles of atmospheric boundary layer physics should provide the reader with the background needed to understand the principles, as well as their importance, used in this work.
The wind tunnel measurements are described carefully in the chapter three, to give an idea about the problems that are encountered if proceeding quality checks of pre-calibrated ultrasonic anemometers. The basic behaviour of an ultrasonic anemometer in a laminar flow and the importance of the neglected vertical component are shown as well.
In the chapter four the enhancement of the calibration is described, showing the advantages that can be used to optimize such a procedure.
Chapter five provides a description of the measurement site and a quality control of the measurement data.
Afterwards, in chapter six the fluxes derived from the measurement data are presented, giving an idea about how much the enhancement of the calibrations improves the measurement and also showing general atmospheric behaviour like atmospheric stability or sensible heat flux for an offshore location.

Chapter 2

Theoretical Background

2.1 Atmospheric Boundary Layer

This chapter should give a brief overview over the basics of principles in atmospheric physics, to highlight why certain parameters are interesting and how to gain them. The briefness results from the fact, that a lot of excellent books (for example Stull (1988), Kaimal (1994)) have been written about atmospheric physics, so there is no need to talk at great length about theoretical basics, which have been presented in a much better way in other works. But to provide the reader with the right context for this work, a few key principles are outlined.

2.1.1 Basics

The part of the atmosphere that is dealt with in this work is the so called surface layer, defined as the lowest 10 $\%$ of the boundary layer. The boundary layer is characterized by the fact that it is influenced by surface processes of the earth with a response time of about an hour. The influence of the surface is mostly due to turbulent processes. For example transport of aerosol, moisture and heat is conducted via turbulence in the atmosphere. These transport processes are best described by fluxes.
To examine turbulent processes, the Reynolds decomposition is used: A signal X consists of a mean part $\overline{X}$ and a turbulent (or perturbation) part x'.

$$X = \overline{X} + x' \tag{2.1}$$

2.1.2 The Logarithmic Wind Profile

While at the ground the wind speed is reduced to zero because of frictional drag, with increasing height the wind speed increases as well because of pressure gradient forces. The variation of the wind speed is nearly logarithmic in statically neutral situations. For other stability situations the wind profile slightly differs.

$$\overline{u}(z) = \frac{u_*}{k} \; ln\left(\frac{z}{z_0}\right) \tag{2.2}$$

Where u_* is the friction velocity (explained in section 2.1.3), k is the von Kármán constant, z the height above the surface and z_0 is the aerodynamic roughness length.

2.1.3 Monin-Obukhov Similarity Theory

With the four Monin-Obukhov key parameters, a relation between the vertical behavior of dimensionless mean flow and turbulence properties within the atmospheric surface layer can be described. These key parameters include:
z: the height above the surface;
$\frac{g}{T_v}$: the buoyancy parameter ratio of inertia and buoyancy forces;
$\frac{\tau}{\rho}$: the kinematic surface stress;
$Q_{v0} = \overline{w'T_{v0}}$the surface virtual temperature flux,
where g is gravitational acceleration, T_v is a virtual temperature, τ_0 is turbulent stress at the surface, ρ is air density, Q_{v0} is a kinematic virtual heat flux at the surface and $\overline{w'T_{v0}}$ is the covariance of the vertical velocity w with the virtual temperature near the surface T_{v0}.
With these parameters a set of scales for the surface layer can be defined. One of these scales, the friction velocity u_*, is of further importance in this work and should therefore be mentioned. It is a measure of turbulent surface stress.

$$u_* = (\overline{u'w'}^2 + \overline{v'w'}^2)^{\frac{1}{4}} \tag{2.3}$$

2.1.4 Atmospheric Stabilities

Atmospheric stability expresses how much the atmosphere is in equilibrium or not. Three main classes can be established:

- **stable:** Warmer air resides over colder air. The area where the two layers meet is called inversion, because usually, air gets colder with rising height. If an air parcel would be lifted out of its original position in stable stratification, it returns to its original position.

- **unstable:** Colder air resides over warmer air. If an air parcel is moved from its original position, it keeps moving in that direction.
- **neutral:** Here the change of temperature with height is identical to the temperature loss due to expansion with increasing height. Thus an air parcel lifted from its original position will stay at its new position.

Atmospheric stability is classified by the Obukhov-Length. This parameter relates dynamic, thermal and buoyant processes:

$$L = \frac{-u_*^3 T_v}{kgQ_{v0}} \tag{2.4}$$

where where k is the von Kármán constant, u_* is the friction velocity, g is the gravitational acceleration, T_v is the virtual temperature, and Q_{v0} is the kinematic virtual temperature flux at the surface. The virtual temperature T_v is the potential temperature that dry air would have if its pressure and density were equal to those of a given sample of moist air. The potential temperature Θ is the temperature that unsaturated dry air would have if brought from its initial state to a standard pressure p_0.
The relation between height above the surface and Obukhov length z/L is zero for statically neutral, positive for stable and negative for unstable stratification.

2.1.5 Fluxes in the Boundary layer

The set of equations build by the Monin-Obukhov similarity theory and the hypothesis that the fluxes in the surface layer are uniform with height help to determine the momentum flux, sensible heat flux, and fluxes of water vapor and other gases, which describe the transport in the atmosphere.

2.2 Measurement of Fluxes

2.2.1 Eddy Correlation Method

The turbulent part of a measured signal is often quite small compared to the mean part and highly fluctuating. It is used in the eddy correlation method, in which fluxes can be described by the correlation of two values.
For the example of heat flux, this connection can be easily illustrated.
Consider two layers of air, the one on top colder than the other as visualized in fig. 2.1.

A parcel of warmer air from beneath begins to rise into the layer of colder air. The relative temperature is positive, because the surrounding air is colder and

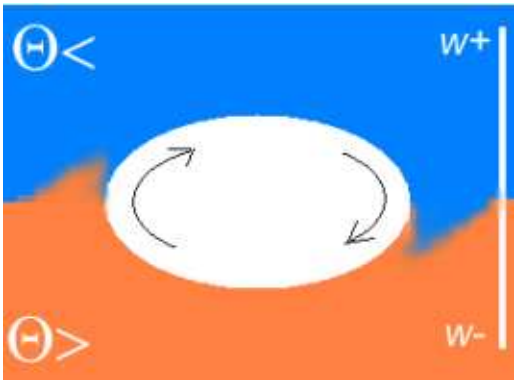

Figure 2.1: Two layers of air differing in temperature. Movement of air parcels up and down.

the relative height is positive as well, because the air parcel has risen. For colder air, sinking down into the layer of warmer air, the temperature difference and the height difference are both negative for respective reasons. For both movements the product of temperature and height difference results in a positive value, which seems sensible, because heat is transported upwards in both cases. To describe all the flux of heat because of turbulent transport, one can sum up all movements up and down, ending in the mean value of all temperature and height products. This is proportional to the heat flux.

$$HeatFlux \sim \overline{w'\Theta'} \tag{2.5}$$

Because of the high fluctuation of the used turbulent component, high resolution measurements are crucial.

2.2.2 Ultrasonic Anemometers

The standard instrument for wind speed measurements is a cup anemometer, using the drag force of the wind to measure its speed. Cup anemometers usually produce measurement values in intervals of a few seconds, because of the inertia of the device, which can not instantly react to an change in wind speed. This is not sufficient for turbulence measurement which may change much faster. Additionally, cups can only measure the horizontal wind components with one instrument. Another wind speed measuring instrument, the ultrasonic anemometer (further referred to as "sonic"), can measure with a resolution of up to 50 Hz for modern instruments. This is very useful for high resolution flux measurements. Besides, sonics are able to measure the three-dimensional wind vector and the temperature

with one instrument.
A sonic basically consists of transducer pairs, between which ultrasonic sound signals are sent back and forth. The wind component along this path changes the speed of the signal, depending on the signals direction. This leads to a runtime delay between the different directions of the signal. With knowledge of the distance between the transducers, the wind speed of the air volume between the transducers can be calculated, with the runtime delay. If t_1 is the runtime to, t_2 the runtime back to and s is the distance between the transducers, the wind speed v can be calculated as follows:

$$v = \frac{s}{2}(\frac{1}{t_1} - \frac{1}{t_2}) \tag{2.6}$$

If three different linear independent measurement paths are used, a three dimensional measurement is possible.
While the lack of moving parts make them low-maintenance instruments, each sonic has to be calibrated carefully. The supporting structure and the transducer heads of the sonic do influence the air flow in the measurement volume. This has to be considered if measurement data of ultrasonic anemometers are used.

2.2.3 Calibration of Ultrasonic Anemometers

As mentioned, the supporting structure and the transducer pairs of the sonic flaw the measurement. Fig. 2.2 gives a close look at the disturbing probe head. A measurement made with an uncalibrated sonic is shown by fig. 2.3. The symmetry of the probe head with the three struts positioned in 120 degree steps clearly shows. Deviations up to 10 $\%$ from the actual wind speed are found. This clearly indicates the need for correction of the raw sonic data.

Flow Distortion in the Instrument

In the course of ultrasonic anemometer development, several studies in the possibilities of calibration were made.
Wiesner (2001) and Wyngaard/Zhang (1985) focused on the disturbing influence of the transducer design. The sensors of the sonics used in this work, which will be described in section 2.2.1, are streamline-shaped. They showed that the so called transducer shadowing effect caused by streamline-shaped transducers is very small in comparison to the flow distortion made by the whole sonic. Thus their effect can be neglected.
Other studies deal with the disturbance caused by the sonic itself. A method used by Grelle and Lindroth (1994) seems to work quite well in all three spatial directions. They use a representation of the distorted component of the wind vector

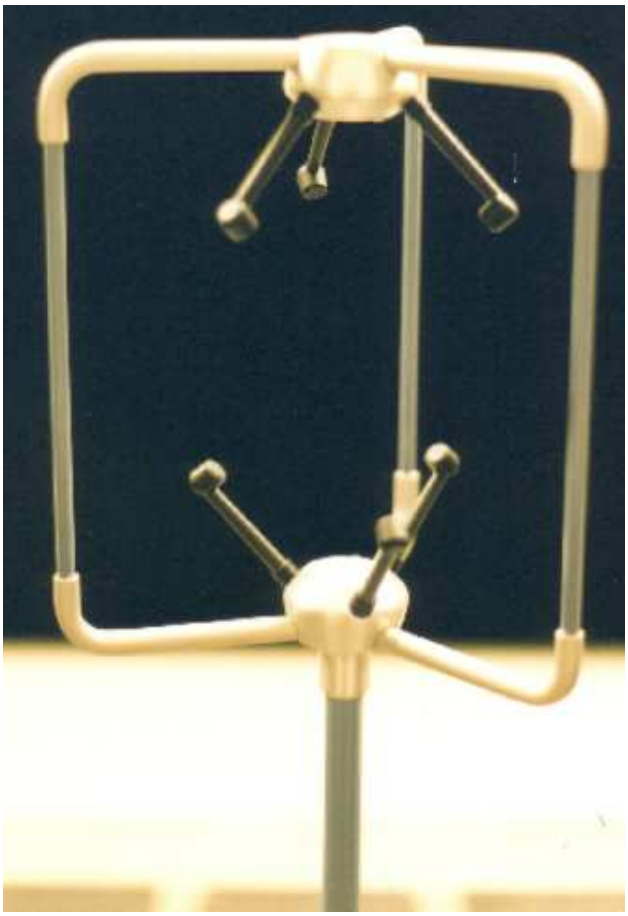

Figure 2.2: Probe head of the employed ultrasonic anemometers. Position of the transducer pairs and the supporting struts can be easily seen.

by a linear combination of the undistorted wind components and specific coefficients as developed by Rotach (1991). These linear combinations build a system of equations, which in matrix notation has a coefficient matrix. To calculate these matrix coefficients, a system of linear equations using theoretical and measured wind components has to be solved.
Others (for example BUBBLE (2004)) used a specific correction matrix, directly based on measurement data from a calibration measurement in a wind tunnel, compared to a reference measurement, usually recorded with pitot tubes. This method is similar to the one Gill uses (see section 3.2.1.2), but features a wider range of spatial configurations.

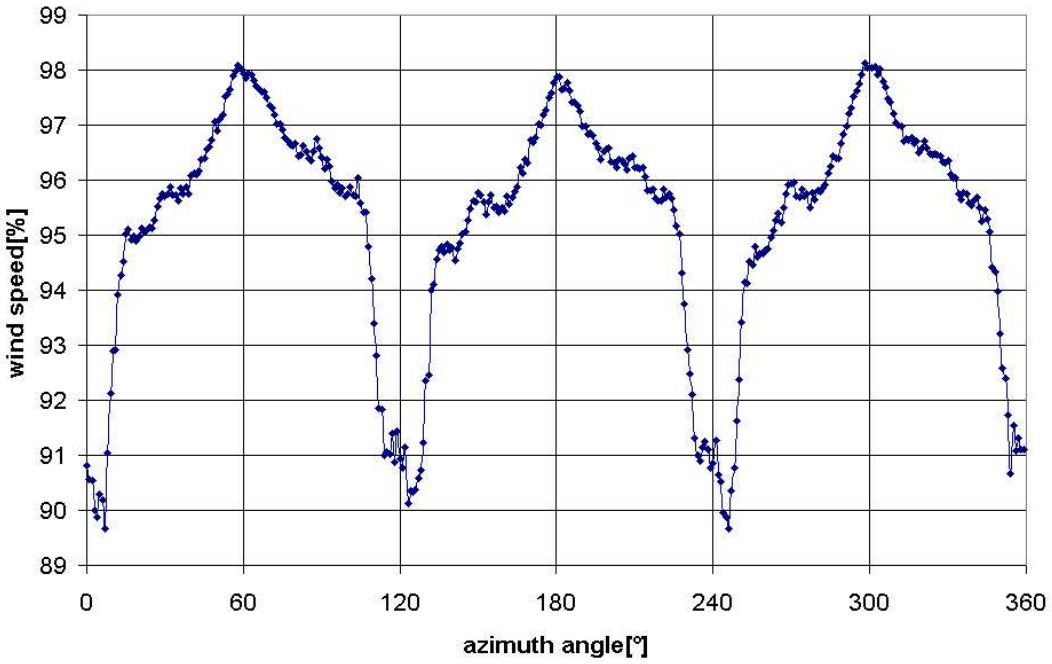

Figure 2.3: Measured wind speed as a percentage of the reference wind speed over azimuth angle. Uncorrected measurement values.

Correction of Mounting Errors

Some methods especially consider possible errors through tilting of the sonic. For a long time the disturbed flow field for wind speeds with a vertical component was corrected by a so called "tilt correction" (Kaimal et al., 1969) which uses a coordinate transformation to adjust the measured values.
Based on the discovery that the "tilt correction" method was incorrect (see Wyngaard (1981)), new ways to represent the disturbed wind flux were found by him, and an alternative calibration method was evolved by Rotach (1991). Wilczak (2000) compares three different techniques for a tilt correction, resulting in the conclusion that the method of "Planar Fit", which is explained later on, is preferable, if working on a flat surface, which is given at offshore locations.
Gash and Dolman (2003) developed an enhancement for an already calibrated sonic, for elevation angles larger than 20 degrees.
Most of these methods require quite an amount of measurement data to be applied. Grelle and Lindroth measured a full rotation under elevation angles from -10 to 10 degrees for a wind speed of 2 to 8 m/s. In the BUBBLE project, a full rotation under eleven different elevation angles between -25 and 25 degrees was

performed at wind speeds from 2 to 8 m/s.

Planar Fit

This method uses a different approach for the tilt correction of an sonic anemometer. Basically the mean streamline field is compared to the mean sonics measurements. For a tilted sonic, the mean streamline values $\overrightarrow{u}_p$ can be obtained by multiplying the measured values $\overrightarrow{u}_m$ with a rotary matrix $\mathbf{P}$, which transforms $\overrightarrow{u}_m$ into the streamline coordinate system. A possible measurement offset $\overrightarrow{c}$ of the sonic has to be considered.

$$\overrightarrow{u}_p = \mathbf{P}(\overrightarrow{u}_m - \overrightarrow{c}) \tag{2.7}$$

The mean wind components are thus:

$$\overline{u}_p = p_{11}(\overline{u}_m - c_1) + p_{12}(\overline{v}_m - c_2) + p_{13}(\overline{w}_m - c_3) \tag{2.8}$$
$$\overline{v}_p = p_{21}(\overline{u}_m - c_1) + p_{22}(\overline{v}_m - c_2) + p_{23}(\overline{w}_m - c_3) \tag{2.9}$$
$$\overline{w}_p = p_{31}(\overline{u}_m - c_1) + p_{32}(\overline{v}_m - c_2) + p_{33}(\overline{w}_m - c_3) \tag{2.10}$$

Because in the mean streamline coordinate system the vertical component $\overline{w_p}$ has to be zero, we can conclude that:

$$\overline{w}_m = c_3 + \frac{p_{31}}{p_{33}}\overline{u}_m - \frac{p_{32}}{p_{33}}\overline{v}_m = b_0 + b_1\overline{u}_m + b_2\overline{v}_m \tag{2.11}$$

Mean values of some length of measurement interval (10 min in this work) are taken and via multiple regression the parameters b_0, b_1 and b_2 are calculated. All components of $\mathbf{P}$ can be derived from these parameters, because of relations between the turning angles and the p coefficients as well as geometrical relations between the p and b coefficients. Detailed formula is given by Wilzcak (2000). Once the rotary matrix has been built, the measurement values can be transformed, and turned in mean wind direction, with a second rotation matrix $\mathbf{M}$:

$$\mathbf{M} = \begin{pmatrix} cos\gamma & sin\gamma & 0 \\ -sin\gamma & cos\gamma & 0 \\ 0 & 0 & 1 \end{pmatrix} \tag{2.12}$$

where $\gamma = tan^{-1}\left(\frac{\overline{v}_p}{\overline{u}_p}\right)$

2.2.4 Translation from Laminar to Turbulent Conditions

What has to be kept in mind is that recent research (Högström and Smedman, 2004) has shown that calibration of sonics with symmetrical probe head (like the

ones used in this experiment) under laminar conditions in a wind tunnel is not necessarily transferable to turbulent measurement conditions in the field. It was found that the wakes behind the supporting struts of the sonic behave differently under laminar and turbulent conditions, and their change in form and size requires a slightly different correction matrix for each of these two conditions. No correction method of this effect is available. In this work the correction obtained at laminar conditions are assumed to be a good approximation to flow distortion in turbulent conditions.

Chapter 3

Wind Tunnel Investigation of the Ultrasonic Anemometers

3.1 Introduction

In chapter 1 it was shown that sonics need to be carefully calibrated, because of the flow distortion produced by the supporting structure. Although the sonics used are already provided with a factory-installed calibration, it is still important to investigate the quality and validity of this calibration.

Therefore in this chapter, the sonics used on the research platform are investigated in the wind tunnel before installation. The aim is to detect and correct possible errors in the factory-installed calibration. The main focus is on the fact that the factory installed calibration of the sonic was developed only for the horizontal components and no tilting was considered. Deviations caused by a vertical tilt should be observed carefully.

Because of the time schedule for installation on the platform, only very limited time was available for the wind tunnel measurements. Therefore a calibration method was developed, which needed only few measurements.
The variables important for an investigation are the angle of attack (azimuth angle ϕ), the tilting angle (elevation angle θ) and the wind speed (U). These variables can be varied in the wind tunnel test setup and contribute to the behaviour of the sonic.
Variation of these variables in a resolution of 1 degree and 1 m/s steps leads to nearly half a million measurements for the characterization of one sonic. Even with an automated measurement process, this is impractical and it would be preferable if the number of measurements needed could be decreased. Therefore pos-

sible symmetries and linear behaviour of the sonic for some of the influencing variables have to be found. This would not only be important for the efficiency of the test measurements, but also for a possible correction of the calibration.

3.2 Experimental Setup

3.2.1 The Ultrasonic Anemometer

Description of the Ultrasonic Anemometer

The sonics used in this work are from Gill Instruments Ltd., model 1210R3-50, SN 255, 273 and 274. They are referred to as #255, #273 and #274 in the following. Their overall height is 0.75 m. The probe head is symmetrical, the three supporting struts are found at 120° steps. A blueprint is shown in fig. 3.1. Specifications are given in table 3.1.

Sonic Model	Gill 1210R3-50
Ultrasonic Sampling Rate	50 Hz
Wind Speed Range and Resolution	0-45 m/s, 0.01 m/s
Wind Speed Accuracy	$< \pm 1\%$ RMS
Wind Direction and Resolution	0-360° , 1°
Wind Direction Accuracy	< ± 1°
Temperature Range	-40° to +60°
Accuracy Range	wind speed < 32 m/s elevation angle < ± 20°

Table 3.1: Specifications of the Gill R3-50, taken from the datasheet provided by Gill Instruments Ltd. (2001)

Calibration of the Gill R3

To calibrate their sonics, Gill uses a purely empirical method. Each sonic is put into a wind tunnel, and for a full rotation at a constant wind speed of 7 m/s the output of the sonic is measured in one degree steps. Only horizontal components are accounted for. These measurement values are compared to the reference speed of the wind tunnel. Deviations are listed in a table for each azimuth angle. This table is used to apply the corresponding correction factor to the measurement value for each azimuth angle. This correction applies only to an elevation angle of zero degree for the sonic, and additionally not for the vertical component. Besides, the

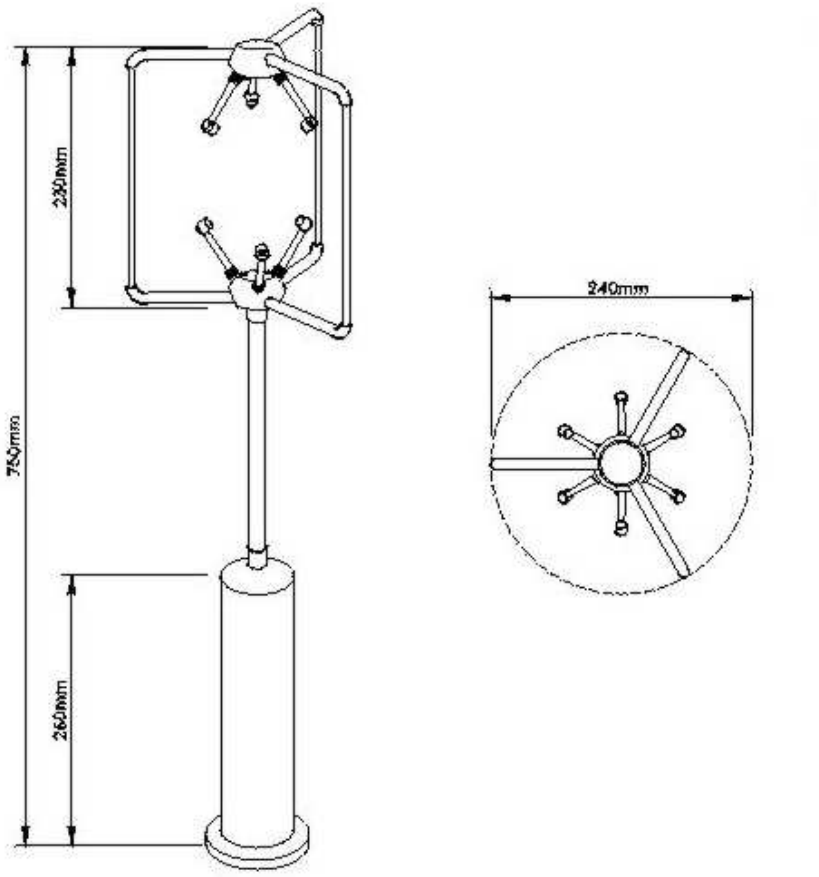

Figure 3.1: Blueprint of the sonic, side and top view. Picture from Gill Instruments Ltd.

deviations are assumed not to change with changing wind speed. Fig. 3.2 shows a measurement of wind speed over wind direction with an applied calibration. Although it is much better than the uncalibrated wind speed over wind direction shown in section 2.2.3, it still has flaws.

3.2.2 Experimental Setup

The measurements were proceeded in the Oldenburg wind tunnel. The wind tunnel has an open measurement volume and a closed circulatory system. The measuring volume is 1.8 x 1,0 x 0,8 m^3. A sketch of the wind tunnel is shown in fig. 3.3. For more detailed information about the wind tunnel see Stabe and Langner (1997)and an internal paper from the Institute for Technical and Applied Physics.

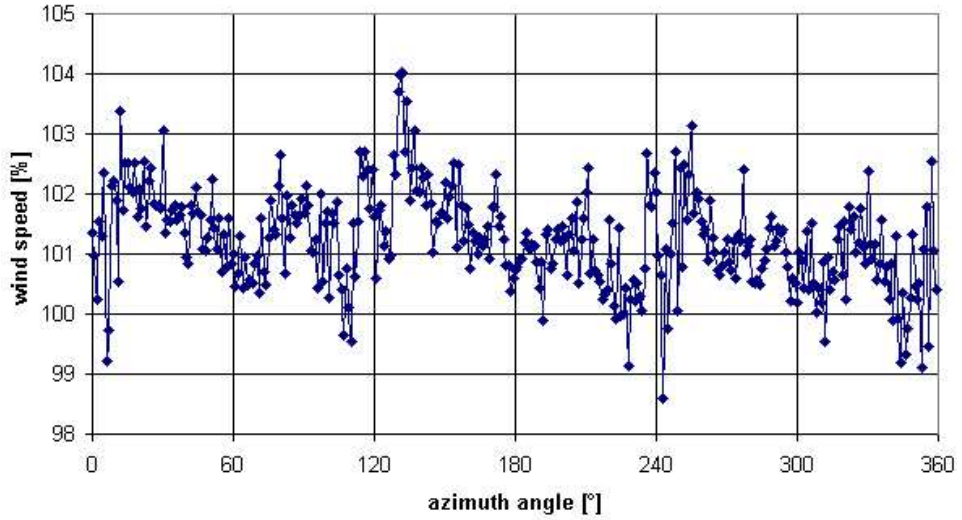

Figure 3.2: Measured wind speed as a percentage of the reference wind speed over azimuth angle. Measurement values corrected by Gill.

The experimental setup is shown in fig. 3.4.

The sonic is mounted on a swivel arm in the open measurement volume, with its north direction pointing away from the wind. The mounting allows a full rotation (360 degrees) in the horizontal plane to change the azimuth angle. Variation of the elevation angle is possible through the swivel arm, allowing tilting angles from -35° to 35°. Four pitot tubes, used for obtaining a reference signal, are mounted at the opening of the wind tunnel. Their pressure signals are converted into voltage signals by electric pressure sensors. The measurement values are registered with a data logger (Ammonit, model P414), which collects other experimental data as well. Sonic and data logger are connected to a PC via a serial port. The logging frequency is 1 Hz for the data logger, 20 Hz for the sonic 255 and 273 and 10 Hz for sonic 274. The data of the sonic are recorded by a software provided by the manufacturer. Certain options for logging can be selected in this software. The following options were used in this work:

- Report Mode: UVW CAL (calibrated measurement - the factory installed calibration was used)
- Selected Average: the logged data is an average of 5 (sonic 255 and 273) or 10 (sonic 274) by the sonic registered measured values.
- Axis Alignment: SPAR (u-component is aligned to north alignment).

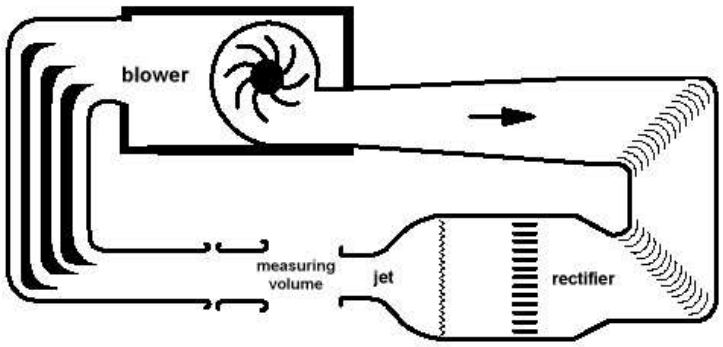

Figure 3.3: Sketch of wind tunnel used for the measurements, taken from an internal paper of the Institute for Technical and Applied Physics

The experimental setup used here was built by Deutsche Windguard GmbH.

3.2.3 Offset Measurement of the Pitot Pressure Sensors

The electronic pressure sensors have a temperature and air pressure dependent offset. Therefore ahead of every measurement an offset measurement is conducted, in order to determine the correct offset for each pressure sensor.
For such an offset measurement, the pitot tubes are covered with protective jackets and the wind tunnel is shut down. The offset for the corresponding pressure sensor value is taken from the mean value of each pitot tube measurement.

Pitot tube: Quality of Offset Measurement

The quality of a offset measurement is determined before it is applied. For this the standard deviation of the series of measurements for each pitot tube is considered. A stable measurement is indicated by a standard deviation below 2.5 hPa.
Larger standard deviations lead to differences in wind speed of over 0.1 m/s. Pitot tubes with data showing a standard deviation above 2.5 hPa, are simply taken out of the analysis, because tests have shown that a correction of the deviating tubes is not easily obtained.

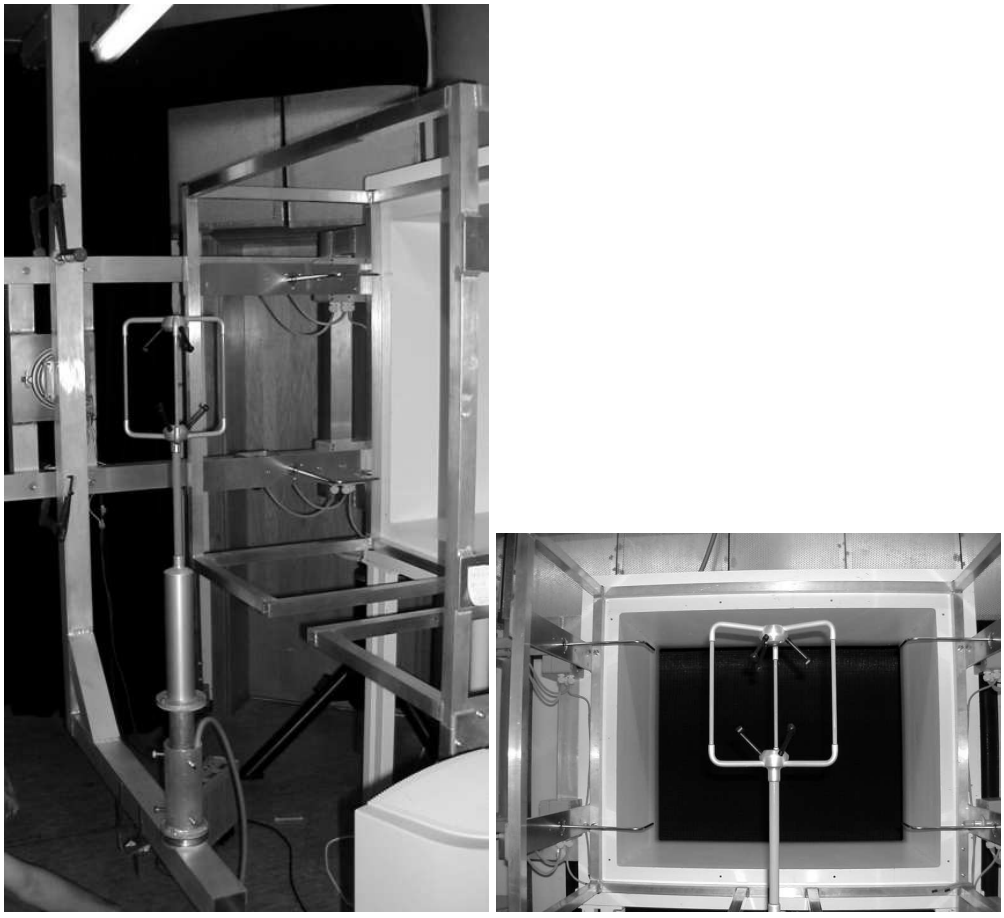

Figure 3.4: Test setup of the sonic in the wind tunnel. To the left mounting of the sonic on the swivel arm, to the right details of the position of the sonic head and the pitot tubes in the wind tunnel.

3.2.4 Data Collection

After determination of the pressure sensor offset the desired wind speed is adjusted in the wind tunnel with the sonic still in north alignment. In this position, the flow distortion of the instrument is smallest. Then azimuth and elevation angle of the sonic are set to the according values. When the airflow has stabilized again, the measurement of the sonic data begins. The measurement lasts at least for 30 seconds and is logged directly on the computer. Pitot tube measurements are collected with the data logger. They are downloaded at the end of a measurement series. For the assignment of sonic measurement to the corresponding time period in the data logger file, an indicating signal is used. This is switched on during the

measurement period and logged in the data logger as well.

To reconstruct the 3-dimensional wind field, all spatial directions have to be measured. Due to the limited time available for the calibration, only certain selected space angles are measured, from which one can reconstruct a behaviour for the wind flow in all spatial directions.
A complete horizontal rotation (variation of azimuth angle ϕ) with an elevation angle of zero degree is taken at a wind speed of 10 m/s for every sonic. Additionally, certain sectors of the sonic where measured with wind speeds of 5, 10 and 15 m/s and elevation angles varying from -15° to 15°. If only a part of the horizontal plane was measured, the measurements always featured a strut in the middle of the horizontal sector.
For elevation angles, which varied from -35° to +35°, two different azimuth angles where used: 0° and 60°(strut facing wind flow).
Because flow behaviour around the struts seem to be the sensitive part in calibration, measurements where focused on the azimuth angles around them. Higher resolution was used there mostly.

Some series of measurement only consider certain sectors in the horizontal plane of the sonic. In fig. 3.5 the used partition of the horizontal plane is shown. In the internal coordination system of the sonic a negative elevation angle indicates

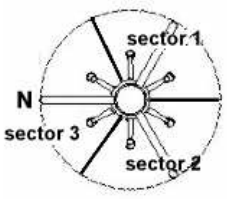

Figure 3.5: Partition of the horizontal plane, N=north alignment

a flow from above, a positive elevation angle indicates flow from below the sonic, see also fig. 3.6.

Wind speed is represented by the magnitude of the wind vector.
In section 3.6 the measurement results are shown. To easily indicate deviations to the expected values, sonic data is displayed as a percentage of the average value of the pitot tubes. If the different sectors of a sonic are measured, the data is plotted sector-wise on top of each other. This representation is chosen, due to the rotational symmetry of the sonic, azimuth angles from 120°-240° and 240°-360°

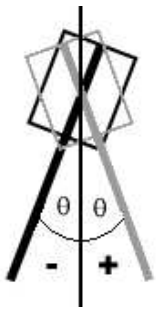

Figure 3.6: Elevation angle direction of the anemometer

correspond to azimuth angles from 0°-120°, as is shown in section 3.7.2.

3.3 Pitot Tube: Measurement of Wind Speed

As mentioned, the pitot tubes are used as a reference signal for the measurement data of the sonics. Hence it is necessary to find a way to calculate wind speed from the measured air pressure. Wind speed and air pressure relate as follows:

$$v = \sqrt{\frac{2p}{\rho}} \tag{3.1}$$

where p is air pressure and ρ is air density.
Air pressure is calculated from each pitot tube measurement, with respect to the acquired offset values and setup specific values given by personal communication with Dieter Westermann:

$$\begin{aligned} p_1 &= (measured\,value - offset) \cdot 15.622 \cdot 0.0049066 \\ p_2 &= (measured\,value - offset) \cdot 15.620 \cdot 0.0049059 \\ p_3 &= (measured\,value - offset) \cdot 15.618 \cdot 0.0049068 \\ p_4 &= (measured\,value - offset) \cdot 15.619 \cdot 0.0049069 \end{aligned}$$

The air density is calculated from several meteorological data collected by the data logger:

$$\rho = \frac{k_1 \cdot p_{air} + \phi \cdot (k_2 \cdot T + k_3)}{T + T_0} \tag{3.2}$$

$k_1 = 0,34844\ kg/m^3 \cdot °C/hPa$
$p_{air} = airpressure[hPa]$
ϕ = relative humidity [%]

$k_2 = -0,00252\ kg/m^3$
$k_3 = 0,020582\ kg/m^3 \cdot °C$
T = temperature [°C]
$T_0 = 273,15°C$

The coefficients k_1 to k_3 are taken from the Deutscher Kalibrierungsdienst (2002).

These parameters are gained as mean values from 30 seconds of measurement. A final correction factor is applied to the mean value of the four pitot measurements. This factor accounts for the change in wind speed because of the expansion of the airflow in the open section of the wind tunnel, as well as the blockage effect the probe head itself causes in the airflow. The correction factor was provided by personal communication with Dieter Westermann (2003).

$$v = (v_1 + v_2 + v_3 + v_4)/4 \cdot 0.9935 \tag{3.3}$$

As a quality control measure, the four pitot tube measurements are compared with each other. If one series of measurements deviates from the others, e.g. does not fit into a range of 0.05 m/s with the other measurements, it is taken out of consideration.

3.4 Fluctuations of Pitot Tube Data at Certain Wind Speeds

Looking at the data of the individual pitot tubes at varying wind speeds reveals a noticeable behavior of the first two pitot tubes in a certain speed range as seen in fig 3.7. For wind speeds from 7 to 10 m/s, the series of measurements shows a periodic oscillation, with a frequency of approx. 0,33 Hz (see fig.3.8). The frequency subsides with increasing wind speed. The strongest oscillation is observed between 8 and 10 m/s, at 7 m/s the oscillation is still perceivable in the standard deviation, while for 11 m/s no difference in the standard deviations for the data of all four pitot tubes can be seen.

With increasing wind speed, all pitot tubes record strongly fluctuating data, but only for the range from 7 to 10 m/s the data of the first two pitot tubes features the described prominent deviation. At other wind speeds the fluctuation is not periodical.

However the mean value measured by the pitot tubes is not altered. Deviations of the mean value are only about 0,01 m/s from the mean value of the data of all pitot

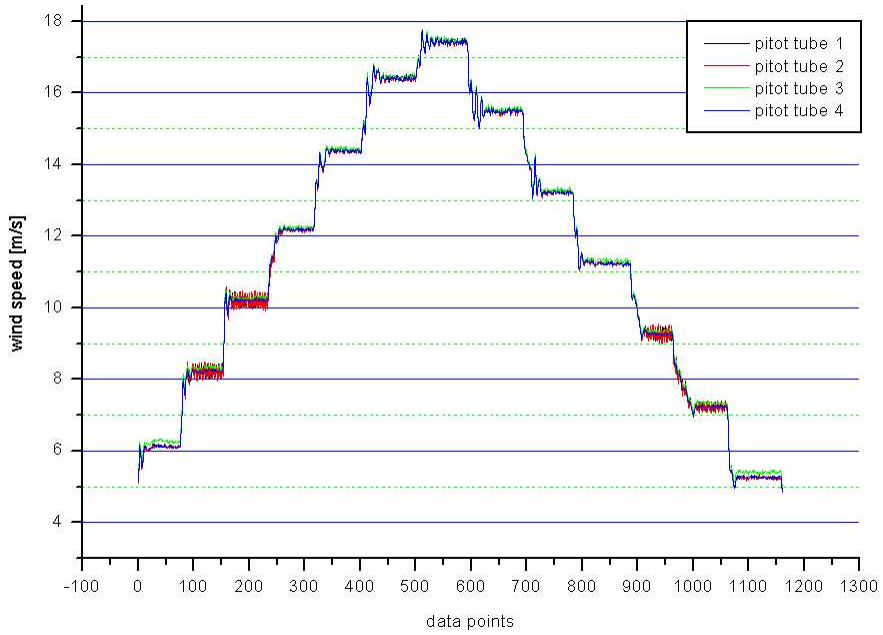

Figure 3.7: Plot of wind speed vs. time for different wind speeds, oscillation of the pitot tube data can clearly be seen for wind speeds from 7-10 m/s

tubes. Therefore the observed effect does not alter the collected data significantly. A possible explanation for these phenomena is that the pitot tubes possess a natural frequency of approx. 30 Hz, the sampling with 10 Hz leads to undersampling, which results in an altered signal with possibly the detected frequency. Tests have shown that the effect disappears if the oscillation of the pitot tubes is prevented (personal communication with Dieter Westermann (2003)).
It should be mentioned that the position of the pressure sensor influences the periodical oscillation as well. It is possible that electrical disturbances play their part in producing this effect.

3.5 Measurement Uncertainty

It is in the nature of measurements that they can not be absolutely accurate. Some possible uncertainties, which have to be considered, are listed here.

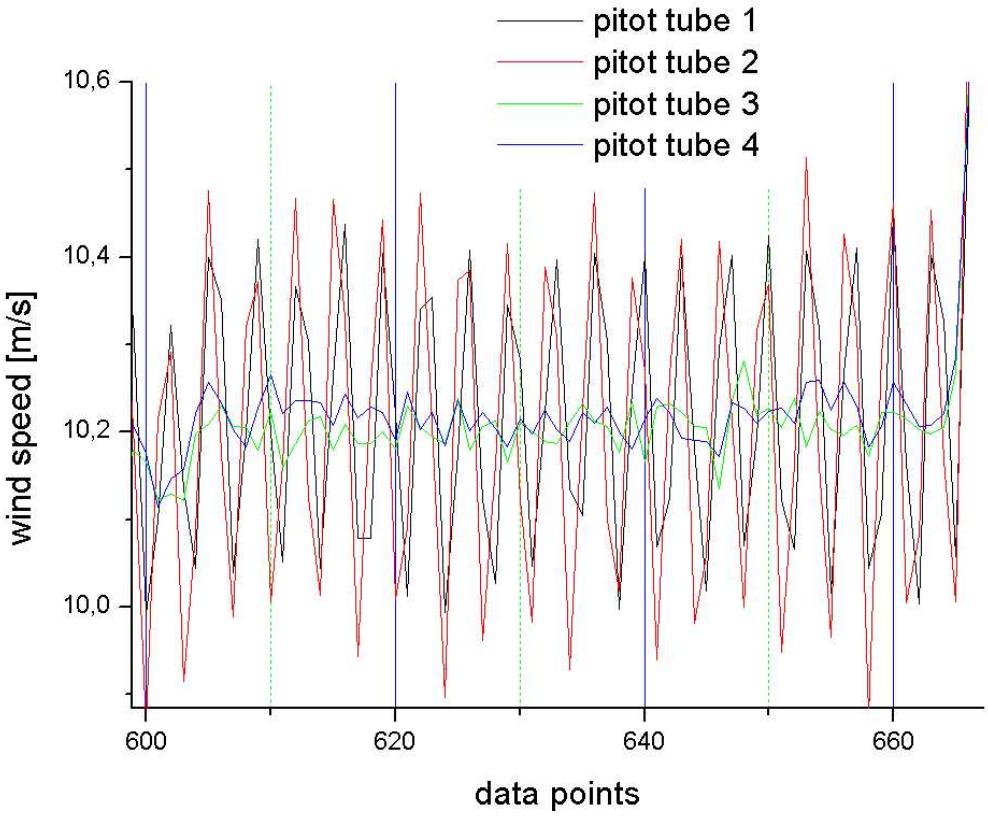

Figure 3.8: Wind speed vs. time for a wind speed of 10 m/s, pitot tubes one and two show a periodic oscillation

3.5.1 Accuracy of Pitot Tubes

Because the pitot tube measurements are going to be used as a reference, the measurement data gained has to be accurate. As mentioned in section 3.3, the reference wind speed is calculated from the measured air pressure and air density (see equation (3.1)). Because the air density is influenced by temperature, air humidity and air pressure, uncertainties in these parameters have to be considered as well. Via error propagation the uncertainty of the wind speed calculation shows to be as follows:

$$\Delta u = \sqrt{\left(\left(\frac{\partial u}{\partial(\Delta p)}\right)\cdot\Delta p\right)^2+\left(\left(\frac{\partial u}{\partial \rho}\right)\cdot\Delta\rho\right)^2}$$

$$\Delta\rho = \sqrt{\left(\left(\frac{\partial \rho}{\partial(p)}\right)\cdot\Delta p\right)^2+\left(\left(\frac{\partial \rho}{\partial T}\right)\cdot\Delta T\right)^2+\left(\left(\frac{\partial \rho}{\partial \phi}\right)\cdot\Delta\phi\right)^2}$$

The partial derivations can be calculated from equations (3.1) and (3.2). For an accuracy of 1 degree/hPa/$\%$ in the temperature/air density/air humidity measurements, an accuracy of 0.2 $\%$ occurs for the measurement of wind speed. These accuracies are realistic for these wind tunnel measurements, resulting in a satisfying accuracy for a reference measurement.

3.5.2 Homogeneity of Wind Tunnel

The air flow produced in the wind tunnel is only valid as a reference wind speed if it is laminar and homogeneous. The homogeneity and hence the quality of the Oldenburg wind tunnel has been verified in measurements made by the Institute for Technical and Applied Physics (ITAP), see Stabe and Langner (1997) for further details. Both deviations from the mean wind speed and turbulence intensity have been measured. Both results are listened in tables 3.2 and 3.3.
A laminar core of the flow is found, depending in size on the distance to the opening. The head of the sonic and the pitot tubes are placed in the laminar core of the flow field, so the pitot tubes can be used as a reference signal.

opening of the wind tunnel [m]	max. deviation [$\%$]	size of core[m^2]
0.14	0.2	0.95 x 0.75
0.5	0.2	0.95 x 0.65
1	0.2	0.85 x 0.55
1.5	0.3	0.75 x 0.5

Table 3.2: Deviations of mean wind speed in the wind tunnel from Stabe and Langner (1997).

opening of the wind tunnel [m]	max. turbulence intensity [$\%$]	size of core[m^2]
0.145	1.2	0.95 x 0.65
0.5	1.3	0.80 x 0.53
1	1.3	0.65 x 0.35
1.5	1.6	0.30 x 0.25

Table 3.3: Turbulence intensity of the wind tunnel from Stabe and Langner (1997)

3.5.3 Mounting Errors of Sonic

Although mounting of a sonic on the swivel arm - or any other supporting structure for that matter - is conducted with great accuracy, there is still a possibility, that

the mounting leaves the sonic not truly vertical or shifted in respect to the north alignment. While a shift in the north alignment can be corrected and is easily seen if one compares the adjusted and measured wind direction of the sonic in a wind tunnel, a tilted sonic must be treated carefully because although its tilt is not easily seen from measurement values, it changes them considerably.
It must be distinguished between a sonic tilted to a vertical axis of rotation and a tilted axis of rotation.
For a sonic which is tilted with regard to the vertical axis of rotation, the deviations expected in all three components are a sine functions. A maximum occurs when the tilt of the sonic amplifies the vertical wind speed, while 180 degrees later, when the tilt attenuates the vertical wind speed (where it can be most clearly seen because of the relatively small value of the vertical component) as the other components as well. Because of the rotation of the sonic, the deviation does not behave linearly between the maxima and minima. One has just to recall the derivation of the sine and cosine function via a vector rotating in the unit circle.
If the axis of rotation itself is tilted instead, a steady offset for the wind speed is expected in all three components, because the axis of rotation and therefore the sensors of the sonic stay in a constant angle to the wind field and the true vertical axis of rotation.
Section 4.4.1 deals with the corrections applied to correct the mounting error in the wind tunnel measurement. In section 2.2.3.2 the correction of this effect in the field measurement is described.

3.5.4 Uncertainties at Low Wind Speeds

As shown in fig. 3.9, measurements below a wind speed of 5 m/s are very imprecise. This results from the measurement range of the pressure sensors and the dependence of wind speed and air pressure. These measurements are neglected in the following study. Above 5 m/s reliable measurements can be made.

3.6 Results

3.6.1 Wind Speed Dependent Response

Wind speeds from 5 to 17 m/s are measured with sonic and pitot tubes in the wind tunnel, a plot of these measurements is shown in fig.3.10. In tab. 3.4 the difference between the reference wind speed and the wind speed measured by the sonics are shown. As can be seen, the measured wind speed exceeds the allowed deviation of 1% of the actual wind speed for the sonics $\#273$ and $\#274$.

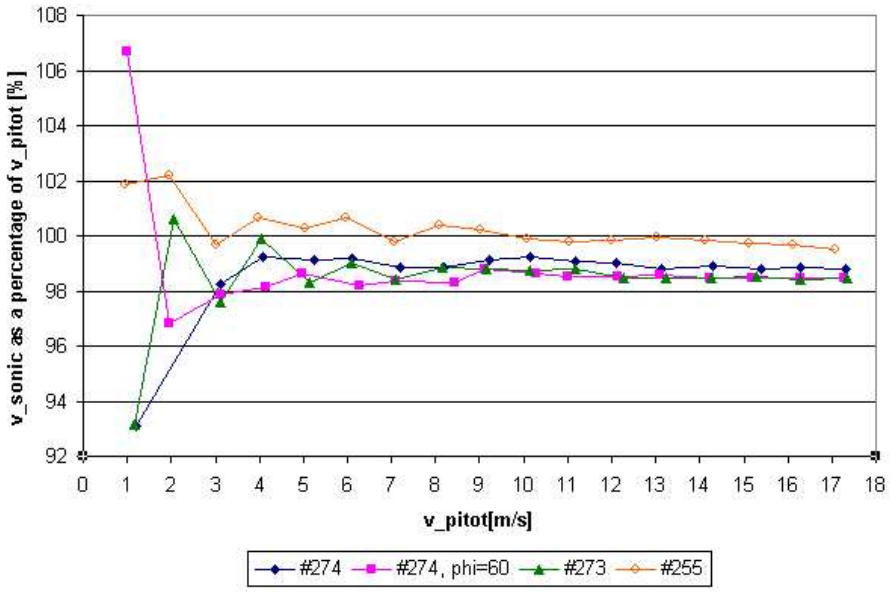

Figure 3.9: Wind speeds of all sonics as a percentage of the wind speed measured by the pitot tubes, for wind speeds from 1 to 17 m/s. For wind speeds below 5 m/s the accuracy of the measurements is very bad.

3.6.2 Azimuth Angle Dependent Response: Horizontal Component

No Elevation Angle

For wind speeds of 5, 10 and 15 m/s either a full horizontal rotation or a rotation from 0 to 120 degrees is conducted.
Fig. 3.11 shows the response of a sonic for a full horizontal rotation at 10 m/s for sonic #255 as example. The behaviour of the other two sonics is similar. A strong peak around 12 degrees in front of each strut characterizes the response of all sonics. The ratio between the wind speed measured by the pitot tubes and the sonics lies in a range of a 0.5 % deviation for the other azimuth angles (taken the offset of sonic #273 and # 274 in account).

Positive elevation angle

For a elevation angle of 10 and 15 degrees the sonic is rotated for 360 or 120 degrees.
In a range of $\pm$ 30° around each strut, the sonic data falls off in comparison to

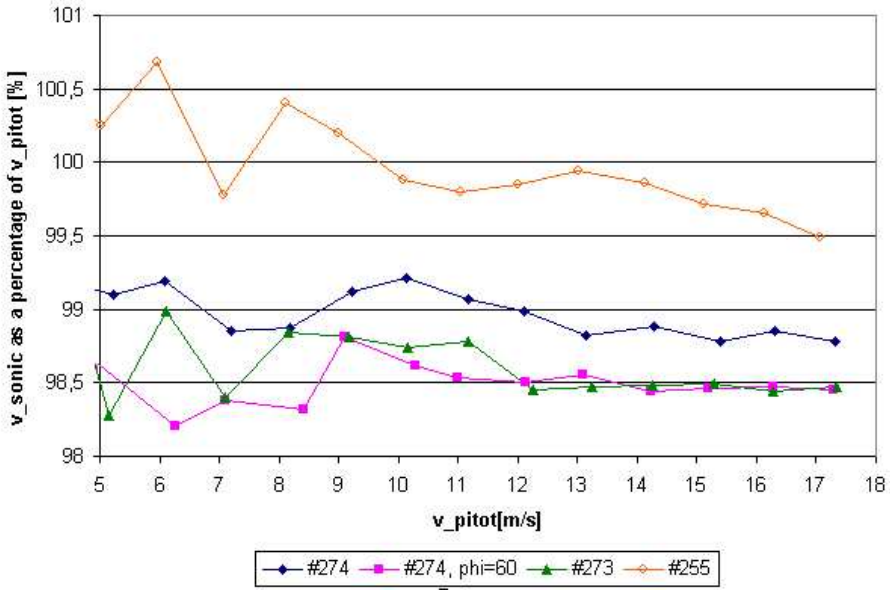

Figure 3.10: Wind speeds of all sonics as a percentage of the wind speed measured by the pitot tubes versus reference wind speed, for wind speeds from 5 to 17 m/s.

the pitot data. The progression of this deviation is characterized by two peaks, between which a minimum lies.
Fig. 3.12 shows measurements made with sonic #273 as example. The same behaviour can also be seen in measurements made with sonic #255 and #274. Comparisons at elevation angles of 10 and 15 degrees show from sonic #273 that the elevation grows with growing elevation angle. See also section 3.6.4.

Negative Elevation Angle

Negative elevation angles of -5°, -10° and -15° are used to observe the response of the sonics for a rotation of 360° or from 0° to 120°.
The data generally features a strong deviation in the range of 10° ahead of each strut. It seems that the deviation increases with ascending wind speed and tilt, though there are differences between the sonics.

Fig. 3.13 shows data for sonic #255, which is exemplary for the experienced response.

sonic	horizontal alignment	difference: sonic / pitot tubes [%] **average value**
#255	0°	**0.48**
#273	0°	**1.41**
#274	0°	**1.05**
#274	60°	**1.51**

Table 3.4: Sonic measured wind speed as a percentage of pitot tube measured, for wind speeds from 5 to 17 m/s.

3.6.3 Azimuth Dependent Response: Vertical Component

Because the vertical component is totally uncorrected from the manufacturer, a special interest lies in the behaviour of this component. Every single measurement shows the same behaviour, an example is shown in fig. 3.14. Deviations of about 0.1 m/s are found for a vertical component when the elevation angle is zero e.g. no vertical component should be existent. At a wind speed of approx. 15 m/s this would lead to a deviation of approx. 0.15 m/s. For the wind speed a linear behaviour can be assumed, as will be shown in section 3.7.2.

3.6.4 Elevation Angle Dependent Response: All Components

For a constant wind speed of 5, 10 or 15 m/s elevation angles from -35° to 35° are adjusted.
In configurations with an azimuth angle of zero degrees, deviations exceeding 1 % of the reference speed only exist for large positive elevation angles, beyond 20 degrees. For an azimuth angle of 60 degrees, stronger deviations are found, for elevation angles smaller than -15 degrees and bigger than 20 degrees. Fig. 3.15 shows the response of sonic #255. On the whole, only for elevation angles having a magnitude of 15 and more degrees significant deviations are registered, these deviations increase with an azimuth angle near 60 degrees.

3.7 Conclusions

3.7.1 Overall Calibration Factor

As presented in section 3.6.1, where the wind speed dependent response of the sonics is shown, it can be seen that the measured wind speed for the sonic #273 and #274 differs for more than 1% of the wind speed measured by the pitot tubes. These observations are consistent with other measurements.

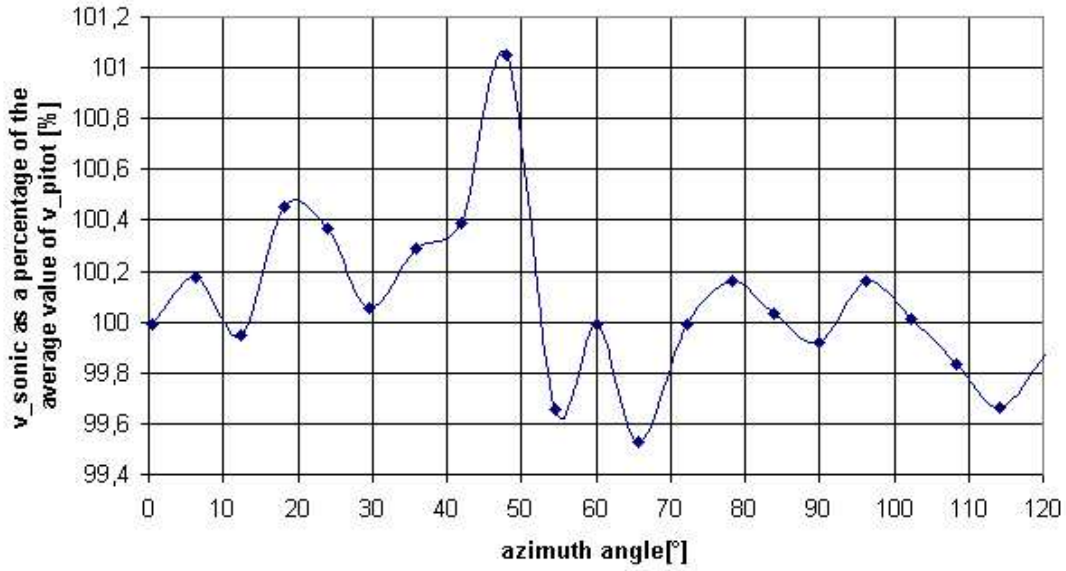

Figure 3.11: Sonic #255: wind speed as a percentage of the reference speed versus azimuth angle, no elevation angle.

As this exceeds the accuracy of wind speed given in the specifications of the sonics (see table 3.1) a correction should be applied to the two sonics.
In case of #273 the overall calibration factor is about 1.41% of the wind speed, for #274 it is 1.05 % far from a strut and 1.51 % near a strut. Although there seems to be a slight wind speed dependence in the overall calibration factor (see figure 3.4), no wind speed dependent overall calibration factor has been chosen, because not enough data is available to verify this dependence.

3.7.2 Symmetries and Linear Behaviour

Variation of Azimuth Angle

The symmetry of the probe head is reflected in a 120° periodic behaviour for the horizontal and vertical components and the magnitude of the wind vector as well, but for reasons of geometry not for the single u and v components which follow a sine respectively cosine function, one wavelength relating to a full rotation. The periodic behaviour is shown in fig. 3.16 for the magnitude of the wind vector. It can be seen that derivations between the different sectors are rather small. The most prominent features are a peak at approximately 48 degrees azimuth angle. These features are visible for all three sections.

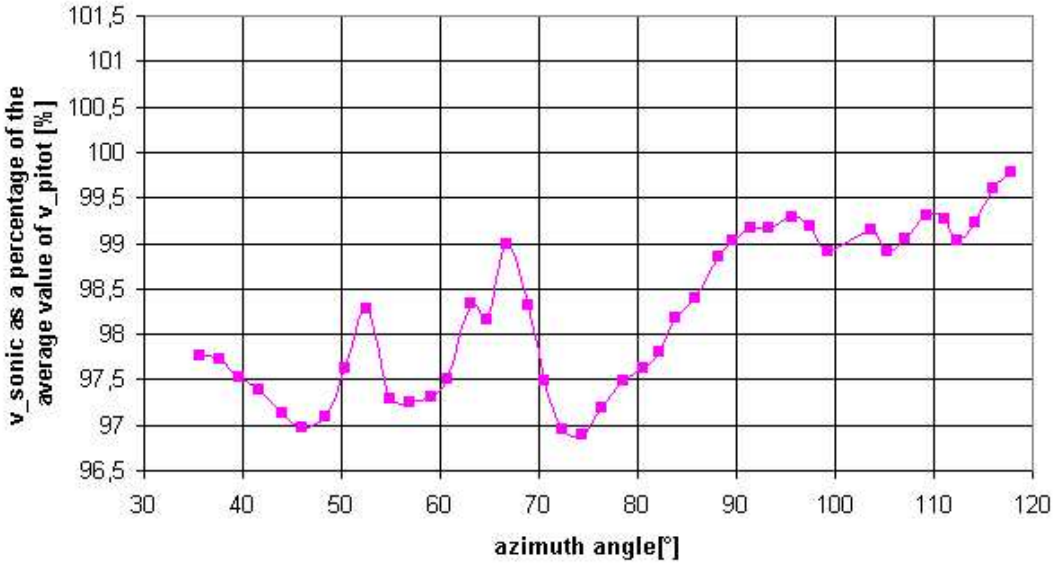

Figure 3.12: Sonic #273: wind speed as a percentage of the reference speed versus azimuth angle, positive elevation angle.

Variation of Elevation Angle

The variation of elevation angles is not symmetric, responses for positive and negative elevation angle differ totally, as can bee seen in section 3.6.2.2 and 3.6.2.3. A possible reason for this is the different position of the sonic in the flow. For a positive elevation angle, the air flows directly over the supporting rod on which the probe head rests. Here the flow is constricted in front of the probe head and widens while passing it, resulting in a lower wind speed than without the disturbance. For a negative elevation angle, the air is constricted while passing the probe head, resulting in a higher wind speed. But a nearly linear behavior between neighbouring elevation angles might be concluded. For the vertical component, another effect can be observed. In fig. 3.17 it can be seen that the elevation angle seems to influence the position of the node of the data. It is shifted towards the position of the strut for positive elevations angles. Only for elevations angles which exceed $\pm$ 10 degrees, this behaviour is clearly shown. It is especially pronounced for an elevation angle of 15 degrees, where every sonics shows a clear shift to higher azimuth angles of the nodes in comparison to other elevation angles. Unfortunately, due to limited time available for the wind tunnel measurements, not enough measurements in this range where made to make a funded statement about a connection between node position and elevation angle.

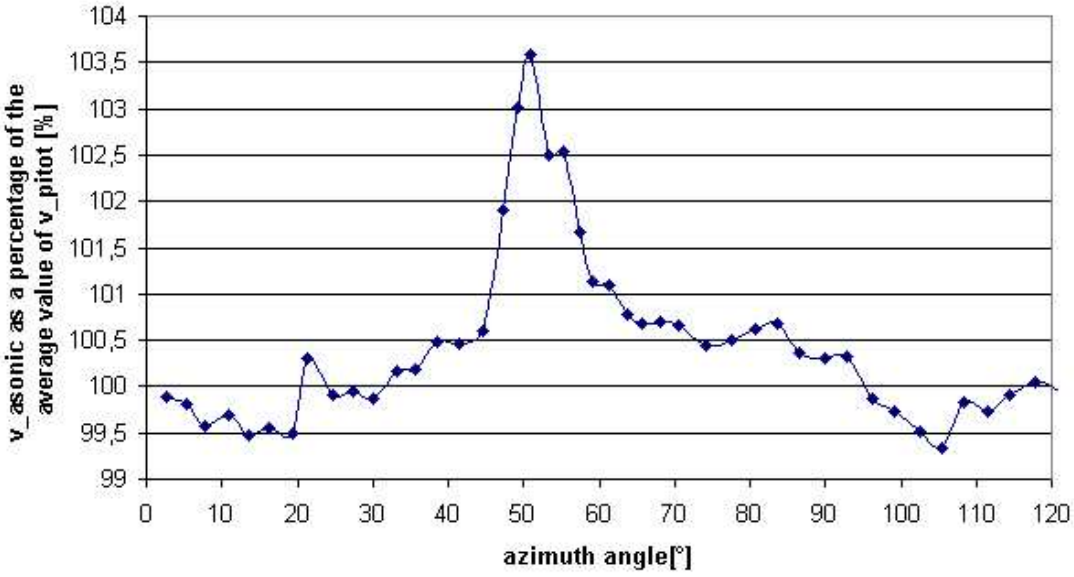

Figure 3.13: Sonic #255: wind speed as a percentage of the reference speed versus azimuth angle, negative elevation angle.

Dependence on Wind Speed

For a laminar flow, the dependence on wind speed is linear. But the flow distortion met here is far from laminar, thus the behaviour of the flow is hard to predict. The turbulent wind field and the wakes, building behind the supporting struts of the anemometer, cause a highly complex process, which can not be described in a linear way.

To investigate how wind speed influences, the vertical component is normalized with the reference wind speed compared for different wind speeds, at a fixed azimuth and elevation angle. The tilt corrected vertical component measured by the sonic is plotted over the reference speed measured by the pitot tubes. For azimuth angles of zero and 60 degrees, several wind speed measurements exist, as already presented in section 3.6.1.

For an azimuth angle of 60 degrees, the behavior resembles a nearly linear behaviour, the sonics response for #274 is shown in fig. 3.18, the sonics #273 and #255 show a similar behaviour.

Based on the measurements made, it is possible to derive an approximate behaviour of the wind speed that meets the observations made. Looking at the phys-

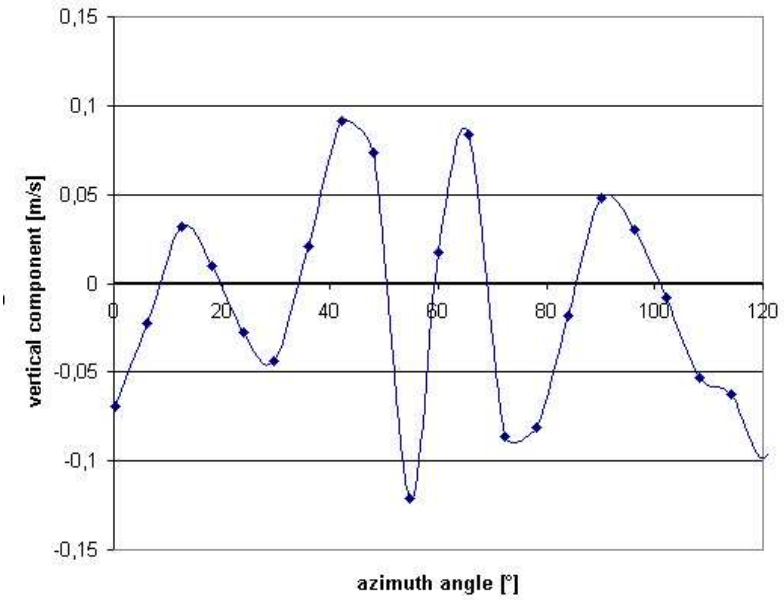

Figure 3.14: #255, vertical component versus azimuth angle for a wind speed of 10 m/s, no elevation angle

ical background describing these phenomena reveals a highly complex theory. No trivial theoretical solution can be found quickly, a sufficient analysis would exceed the scope of this work by far. Because empirical and theoretical methods to find a solution show to be problematic, at least an approximate description of the behavior observed is quite satisfying. The simplest solution is a linear influence of wind speed. For azimuth angles of strong deviation, this solution meets the observations made nearly perfectly as seen in fig. 3.18. If vertical components of different azimuth angles and wind speeds are normalised with the reference wind speed, the result is quite convincing, as can be seen in fig. 3.19.

3.7.3 Deviations

The results for all three sonics investigated are consistent. Comparisons between different series of measurements at points of similar configuration result in correspondence.
Deviations are found around the struts. For no or negative elevation angle, a strong peak ahead of the strut is found, which increases with growing elevation angle, seen if data in section 3.6.2.1 is compared to 3.6.2.3. For positive elevation angles, a symmetrical deviation is found around the strut, which does not depend so clearly on the magnitude of the elevation angle (compare 3.6.2.2).

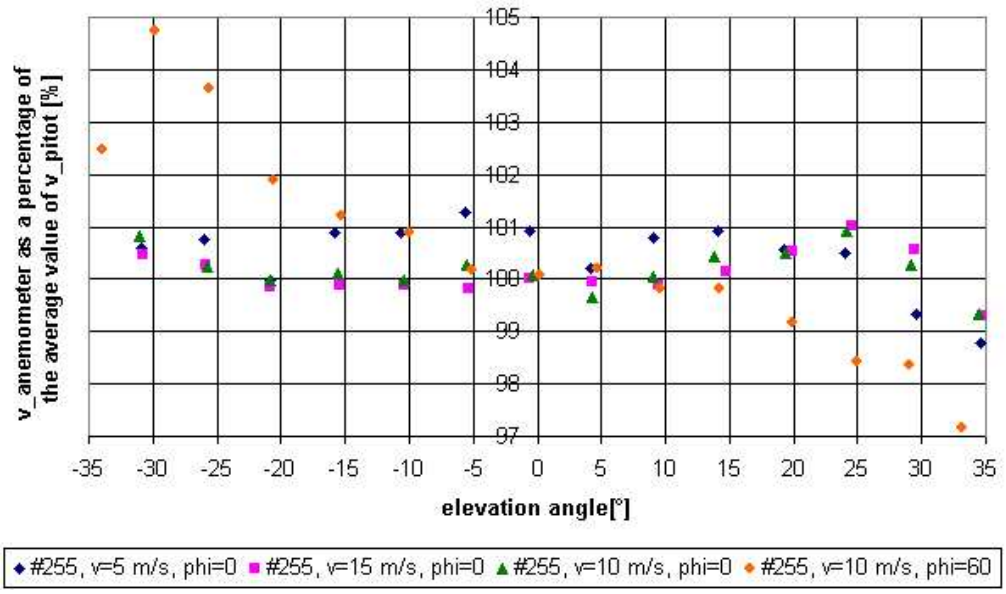

Figure 3.15: Sonic # 255: wind speed as a percentage of reference speed versus elevation angle, variation of elevation angle for different wind speeds.

The disturbing influence of the strut can also be seen in section 3.6.4, where the response shows a totally different behaviour for azimuth angles of 60 degrees. Although variation of the elevation angle shows no strong deviations for elevation angles of magnitude equal or smaller than 15 degrees, it can be observed in section 3.6.2.3 that even smaller elevations angles lead to an increasing deviation.
The third dimension, which is not considered in the factory installed calibration, influences the calibrated measured data which makes a re-calibration necessary. Even for a 2-dimensional measurement constellation the deviations rise above the allowed 1% of the wind speed, since the perturbation caused by the struts is not completely corrected by the factory installed calibration. For the vertical wind speed it is seen that it has to be corrected as well.

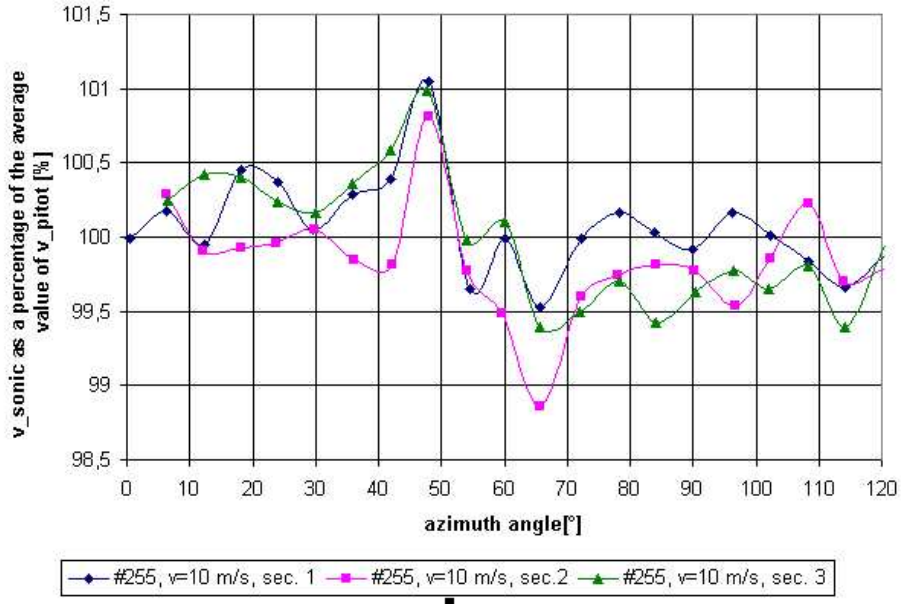

Figure 3.16: Sonic # 255: wind speed as a percentage of reference speed versus azimuth angle for all three sectors of the sonic, wind speed 10 m/s, no elevation angle.

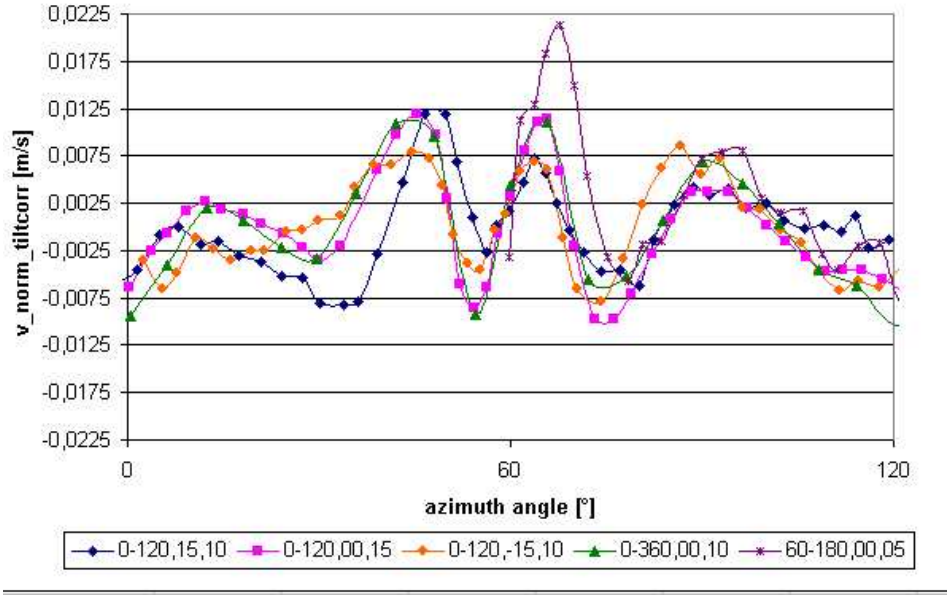

Figure 3.17: Sonic #255: tilt corrected and normalized vertical component versus azimuth angle for different wind speeds.

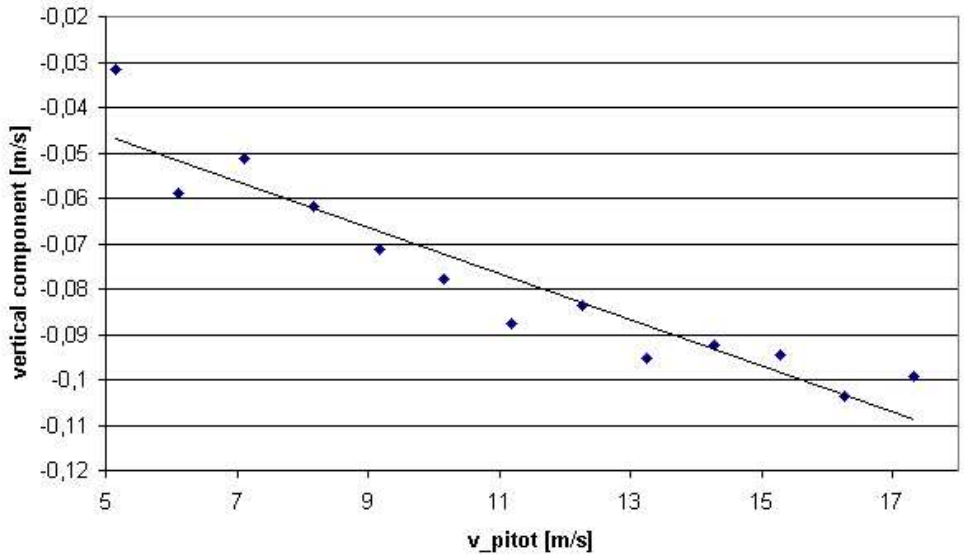

Figure 3.18: Sonic #274: vertical component versus v_{pitot}, azimuth angle of 60°, elevation angle of zero. The solid line shows a linear fit of the measurement data.

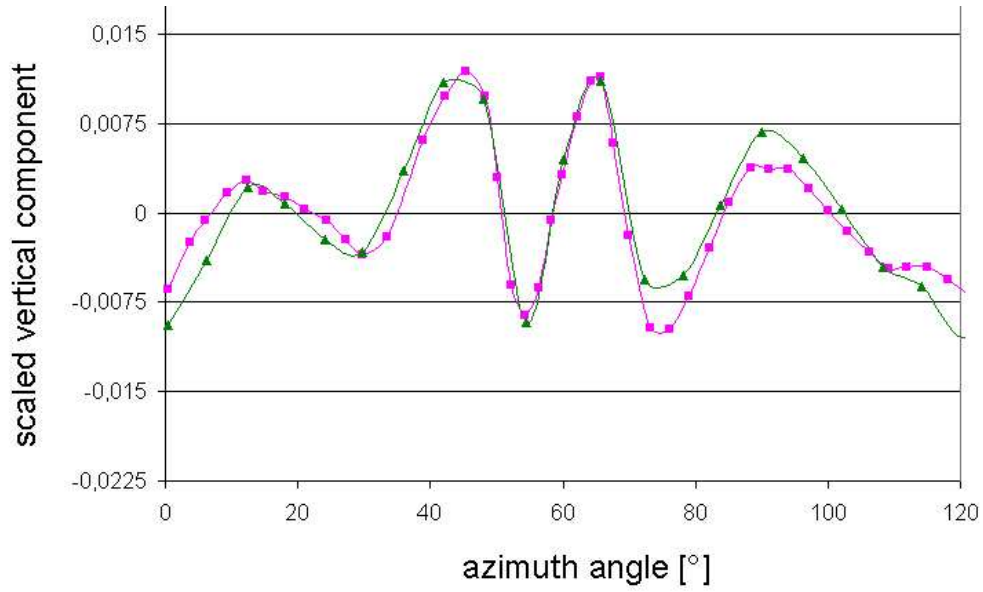

Figure 3.19: Sonic #255: normalized vertical component versus azimuth angle, no elevation angle, triangles were scaled from 10 m/s, squares from 15 m/s

3.8 Outlook

A few phenomena occurred, which were not discussed furthermore in this thesis, but might be of interest:

- The oscillation in the pitot tube data as described in section 3.4: Although the natural frequency seems to be the source of this phenomenon, still electrical effects were found to influence as well. It might be worth to investigate, whether electro-magnetic effects of the experimental setup influence in a disturbing way.
- A deviation of the adjusted azimuth angle and the azimuth angle measured by the sonic was found. Because the measured angle showed more homogeneous data, these values were used. Possibilities for this difference might be a slight misalignment of the anemometer in the setup, or imprecise adjustment of the azimuth angle in the measurements.
- The node shift of the vertical component observed for different elevation angles should be investigated more closely. A connection between these could provide helpful information for further correction of the sonic.
- Although the wind speed dependence could be assumed as linear as a first approximation, a more complex investigation should get closer to the actual behaviour.
- As a recommendation for future measurements: Multiple measurements should be conducted to minimize measurement errors. Additionally it is advantageous to use the same configuration for different sonics, and to measure the full scope of 120 degrees, with a fine resolution around the struts.
- Automation of the measurement setup improves the measurements a great deal.

Chapter 4

Calibration of the Ultrasonic Anemometers

4.1 Introduction

It has been shown in Chapter 2 that a correction and extension of the factory installed calibration are necessary.
Most correction methods need a large amount of measurement data (see Chapter 2.2.3). Because of time limitations extensive measurements where not possible, a calibration method was developed which requires less measurements. Additionally the method has to base on measurements not on a physical description of the flow effects around the sonic. This is because the phenomena found result from physics far too complex to be discussed adequately in this work.

4.2 Description of the Correction Method

The method used here are lookup tables, similar to the method Gill Instruments used, as described in section 3.2.1.2 Unlike Gill, the vertical component as well as elevation angles different from zero where accounted for.
Because of the few measurements necessary, it differs from the methods evolved by Grelle and Lindroth and the BUBBLE project, where much more spatial configurations are needed.
For the tilt correction of the measurement data the method of Planar Fit was chosen, because of the advantages the method provides and because of the number of measurements from the measurement platform will be quite high. The correction of Gash and Polman for large elevation angles was not applied, but elevation angles larger than 20 degrees are very seldom.
For the correction of the flow distortion use was made of the 120 degree sym-

metry of the probe head for the spatial components, as well as the approximately linear behaviour for different wind speeds. For positive, negative and no elevation angles, different lookup tables are used (see chapter 2). So for each sonic exist nine lookup tables: a set of three for each positive, negative and no elevation angle. For each distinct elevation orientation, a correction table for horizontal and vertical components as well as the azimuth angle exist. The usage of the 120 degree symmetry reduces the measurements to one third for each azimuth dependent measurement, the linearity of wind speed makes it possible to use only one representative wind speed and for different elevation angles, only prominent configurations for a positive and negative elevation angle and a configuration for no elevation angle have to be used.
The lookup tables contain the correction factor which has to be applied to the normalized measurement value, according to the current azimuth angle and elevation angle.

The complete correction process is described in the following.

1. At first the three components (u,v,w) of the wind vector are corrected for tilt errors with the Planar Fit method.
2. The wind vector is turned into the main wind direction.
3. Detrending of the wind vectors three spatial components is conducted.
4. Then the wind vector is split up in its horizontal and vertical spatial components and the wind direction is derived, to make use of the 120 degrees symmetry of the probe head.
5. The appropriate correction values are looked up, and scaled to the correct wind speed.
6. The correction is applied to the measurement value.
7. After this correction, the two horizontal (u,v) components are derived from horizontal wind speed wind direction.
8. A fully corrected wind vector exists.

As can be seen, the whole correction process can be separated in three components: tilt correction, detrending and flow distortion correction.

4.3 Detrending

While the method of Planar Fit and flow distortion correction have already been discussed, an important component the "detrending" has to be explained still:
Only the turbulent part of the measurement is of interest in flux measurements. But because a general rise of the wind speed does not contribute to fluxes, but adds to the difference between a measurement value and the mean value of a measurement interval. It must not be mistaken as a turbulent deviation. Therefore the general trend of the observed variable has to be considered: The trend of the measurement interval is calculated via linear regression. The trend is then subtracted from the measurement, leaving a measurement which deviations are purely turbulent.

4.4 Determination of the Lookup Tables from Wind Tunnel Measurements

The calibration depends, as the measurement itself, on three variables: azimuth angle, elevation angle and wind speed. For the wind speed a nearly linear behaviour could be shown, as well as it was shown that for positive and negative elevation angles different corrections are needed. The correction is linearly dependent on the magnitude of the elevation angle. Thus the three sets of look up tables are for elevation angles of -15, 0 and +15 degrees. For elevation angles exceeding the magnitude of 15 degrees, the correction was not interpolated further, but the correction from the corresponding $\pm$ 15 degree elevation angle was used.

For each sonic, the set of three lookup tables for three different elevation angles is calculated for each of the following components: horizontal wind speed, vertical wind speed and wind direction (=azimuth angle).

Before these lookup tables can be derived from the wind tunnel measurement data, the data itself have to be tilt corrected.

4.4.1 Tilt Correction of Wind Tunnel Data

As described in chapter 2, a possible misalignment of the sonic calls for a correction. The data taken in the wind tunnel feature a sinusoidal behaviour for every measurement. This is especially obvious, if looking at the vertical component, because of the high deviations in comparison to the small vertical component. Therefore we can assume that the sonic is slightly tilted to a vertical axis of rotation. Differences of approximately one degree in the vertical angle lead to differ-

ences of 0,1-0,2 m/s in the vertical component. To correct this, the theoretically expected sine function is fitted on the measurement data for each sonic. The following function form is used within this fit:

$$y = a \cdot sin(b \cdot x + c) + d \tag{4.1}$$

with specific coefficients a, c and d. The parameter b has the value of 0.01745 and represents the frequency of the sine function, corresponding to the wavelength of 2π, which equals a full rotation. The coefficient d considers the fact that a slight misalignment of the axis of rotation itself has also happened, resulting in a slight offset.
Fig. 4.1 shows the fit for sonic #255 as an example.

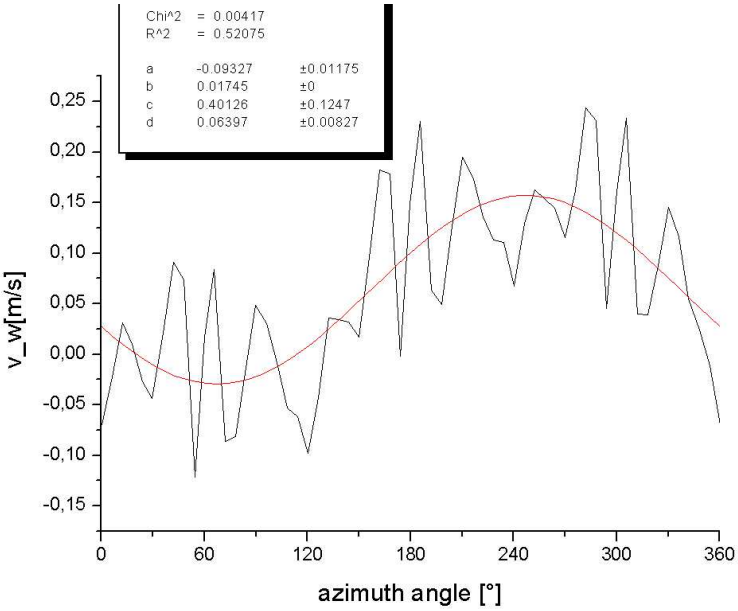

Figure 4.1: Sonic # 255: The vertical component and a fitting function plotted over the azimuth angle, for a measurement with no vertical angle at a wind speed of 10 m/s.

After subtracting these functions, the deviations in all three sectors of the sonic shown to be quite similar, all bearing the same offset from zero, see fig. 4.2. The coefficients found for the three sonics are shown in tab. 4.1. Although it can only be seen clearly for the vertical component, tilt correction must be applied to the other spatial directions as well, because they are also affected by the tilting.

After consideration of the tilt correction the lookup tables can be built. If for certain configurations two or more measurements were made, mean values of these measurements are used.

anemometer	a	a-err	c	c-err	d	d-err
255	0.093	$\pm$ 0.012	3.54	$\pm$ 0.12	0.064	$\pm$ 0.008
273	0.070	$\pm$ 0.012	5.58	$\pm$0.11	0.011	$\pm$0.008
274	0.098	$\pm$0.011	5.65	$\pm$ 0.12	0.008	$\pm$0.008

Table 4.1: Sonic specific coefficients for the tilt correction function. The 2 π periodicity of the fitting functions has been used, thus the difference to the coefficients given in fig. 4.1.

4.4.2 Lookup Table for Horizontal Wind Speed

The magnitude of the measured horizontal wind vector is compared to the reference horizontal wind speed for every azimuth angle and wind speed measured. For this, difference of the wind speed and the vertical component derived from the adjusted elevation angle is subtracted from the reference wind speed. The difference between the reference and the measured wind speed is normalized by the reference wind speed and after that used in the lookup table as a correction value for a normalized wind speed for that azimuth angle. To make use of the 120° degrees symmetry of the probe head, each azimuth angle beyond 120° is subtracted by 120°, respectively 240° if larger than 240°. This procedure also accounts for the steady offset found with sonics # 273 and #274, because the derivation from the reference speed is used.
If more measurements than one are made for a sector, the mean values of the values lying in the same one degree interval are used.

4.4.3 Lookup Table for Wind Direction (=Azimuth Angle)

Because the single horizontal components are calculated from horizontal wind speed and direction, and the measured azimuth angle shows differences to the adjusted one, correction of this variable is necessary as well. Differences of the measured azimuth angle (derived from the two uncorrected horizontal components) and the adjusted azimuth angle are listed in a lookup table. The sonic angle is corrected with these values.

4.4.4 Lookup Table for Vertical Wind Speed

Again, the difference between the reference and the measured wind speed is calculated and normalized with the reference wind speed. The reference wind speed for the vertical component is derived from the geometrical relation between the reference wind speed and the adjusted elevation angle. The mean vertical wind

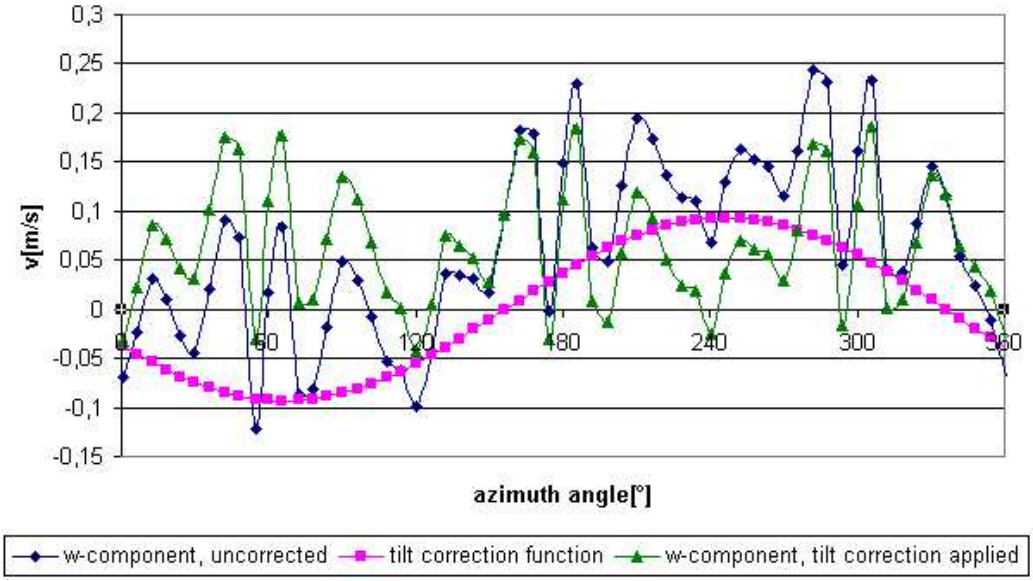

Figure 4.2: Sonic #255: The vertical component with and without tilt correction, for a measurement with no vertical angle, at a wind speed of 10 m/s. No offset applied for better visualization.

speed is added or subtracted, emulating an elevation angle of zero degrees, to enable a better comparison between measurements of different elevation angles.

4.5 Testing of the Calibration Procedure

To test the calibration procedure, an additional measurement was made in the wind tunnel at a constant wind speed of 7.17 m/s with various elevation and azimuth angles. Tab. 4.2 shows the different configurations of azimuth and elevation angle.

After application of the calibration procedure, several improvements can be seen. The mean value of the wind vector decreases from 7.24 to 7.22 m/s, which reduces the overall deviation from 1 % to 0.7 %. Fig. 4.3 shows the difference of the corrected and the uncorrected wind speed. The different correction values used for different elevation angles can be seen very clearly.

The strongest improvement can be seen for the vertical component, where the mean value decreases from 0.08 m/s to 0.06 m/s. Fig. 4.4 shows the differences of a corrected and an uncorrected vertical component. The influence of the different tilt angles on the correction can be clearly seen as well. For a negative tilt angle

azimuth angle	elevation angle
17	00
17	05
17	10
55	10
55	23
100	23
180	23
180	-7
280	-7
280	-21

Table 4.2: Spatial Configurations for the Test Measurement

the difference is heavily fluctuating. This is because the azimuth angle leads to a position in the lookup table with a very steep slope. Thus small variances for azimuth and elevation angles lead to strong differences in the applied correction value.
Generally, for a negative tilt angle, it would be expected to measure a too high vertical component, the procedure should lower the measured value, which it does. And for a positive tilt angle the expected rise of the measured vertical component is found as well. As can be seen, the enhancement of the calibration corrects the measurements in a sensible way and improves the measurements quality.

4.6 Conclusion

- The correction is not perfect e.g. does not reach a 0% error, but for the magnitude reduces the error it had before and for the vertical component lowers it considerably as can be seen in section 4.5

- The calibration method is based on measurements made in a wind tunnel. Possible errors of this measurement are listed in chapter 2. Another problem might be the fact that the behaviour of the flow in the laminar conditioned laboratory can not be exactly transferred to the turbulent conditions met in field measurements. Generally the method can be used for every sonic given, if measurement time is available.

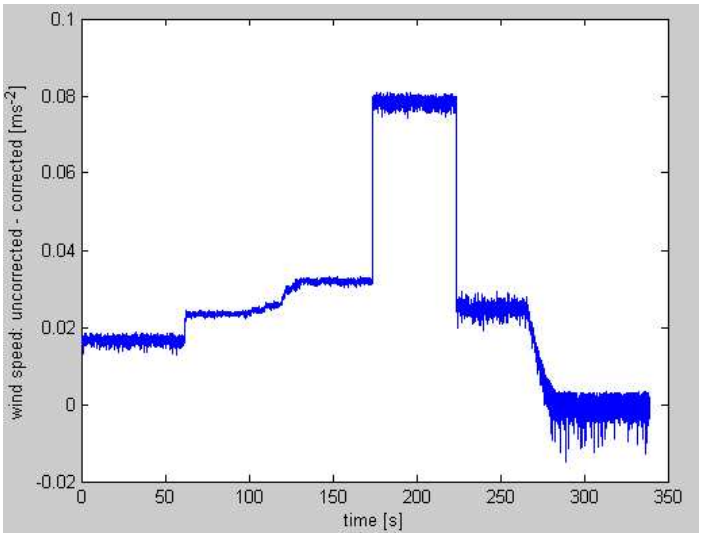

Figure 4.3: Sonic #255: Difference of the uncorrected and corrected wind speed over time.

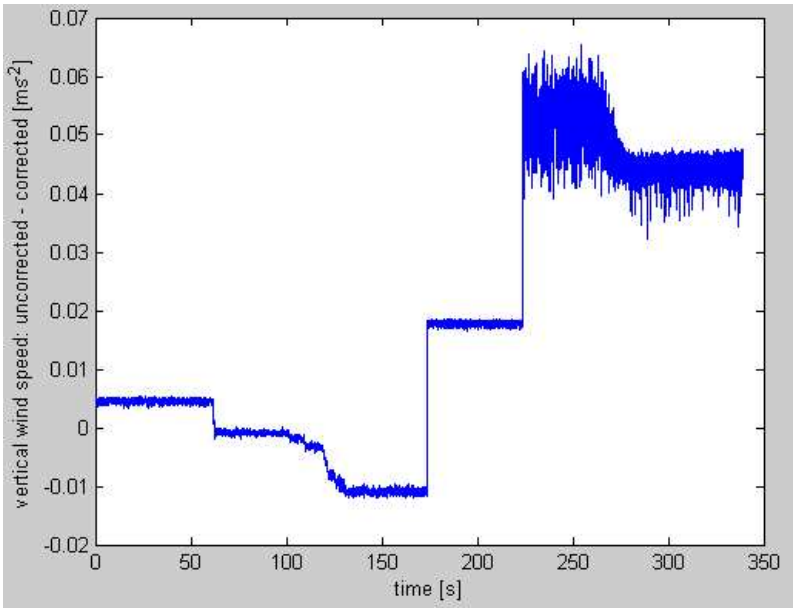

Figure 4.4: Sonic #255: Difference of the uncorrected and corrected vertical wind speed over time.

Chapter 5

The FINO Measurement Platform - Quality Control of Measurements

Before working with the field data gained with the measurement platform FINO, information about the platform and the data collected should be observed carefully. At first, a short description of the platform itself is given, the second section deals with the reliability of the measured data.

5.1 Description of the FINO Measurement Platform

The FINO measurement platform, pictured in fig. 5.2, is located 40 km north of the island Borkum in the Northern Sea, see fig. 5.1. Measurements are available since August 2003, although data of the first month are not very reliable. In this work, data from November 2003 to April 2004 has been used.

The height of the measurement mast is 100m, with seven cantilevers on each side, aligned to north-north-west respectively south-east-east (see fig. 5.3). Sonics, wind vanes and cup anemometers are used for wind speed and direction measurements.

The assembly of the measurement instruments on the mast is as follows: cup anemometes are installed on the one side of the measurement mast on cantilever arms at heights from 30 to 100 meters in 10 m steps. Wind vanes and the sonics where placed alternating on the other side of the mast on cantilever arms, sonics at 40, 60 and 80m, wind vanes at 90, 70, 50 and 30 m height. Additional temperature sensors were placed at 100, 70, 50 and 30 m height. Table 5.1 shows the position of the sonics at the platform.

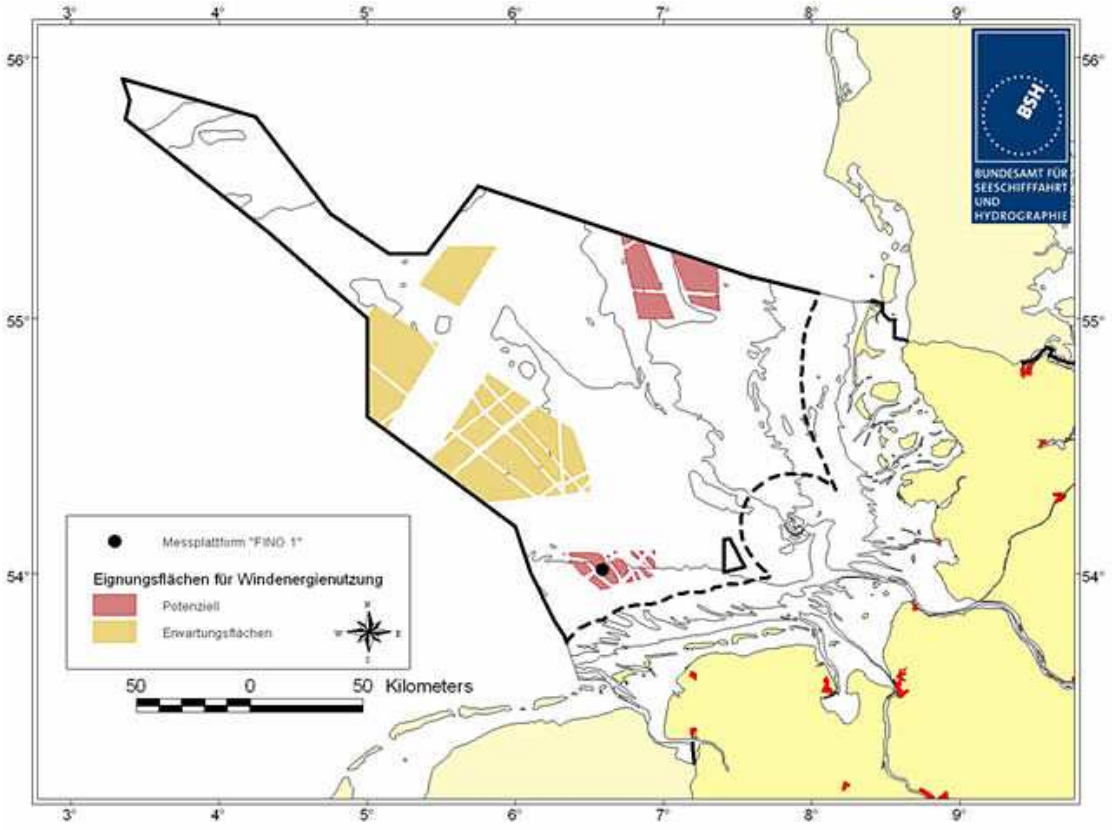

Figure 5.1: Map showing the position of the FINO measurement platform (black dot) in the northern sea, from Germanischer Lloyd WindEnergie GmbH.

5.2 Quality Control of Measurements

The aim of this investigation was to check the correct function of the ultrasonic anemometers. For this purpose data of the sonics are compared to data of the wind vanes for wind direction and to the cup anemometers for wind speed. Before that, the reliability of the reference instruments has to be tested as well.
Measurement data from November, 1st to 30rd 2003 have been used for this comparison. Only measurement data of a minimum wind speed of 7 m/s are used, because of the uncertainties in measurements at lower wind speeds.

5.2.1 Reliability of the Reference Measurements: Wind Speed

Compared to each other, the cup anemometers show a consistent measurement. The ratio between two measurements lies generally between 0.98 and 1.01. If

Figure 5.2: FINO measurement platform in the northern sea, from Germanischer Lloyd WindEnergie GmbH.

greater differences occur, the higher cup anemometer measures a higher wind speed, because of the vertical wind speed profile. In fig. 5.4 these two typical behaviours can be seen. Nevertheless, a few glitches are found. Over all, the measurements seem consistent enough to be used as a reference measurement.

5.2.2 Quality Control of the Sonic Wind Speed

Comparison of the cup and the sonic data shows good concordance, as can be seen in fig. 5.5. The ratio of cup and sonic being for most wind directions nearly one, indicating good concordance. Two strong deviations around 125 and 310 degrees indicate the influence of the measurement mast. For 125 degrees, the wind comes from the cup side of the mast, making the cups measure a much

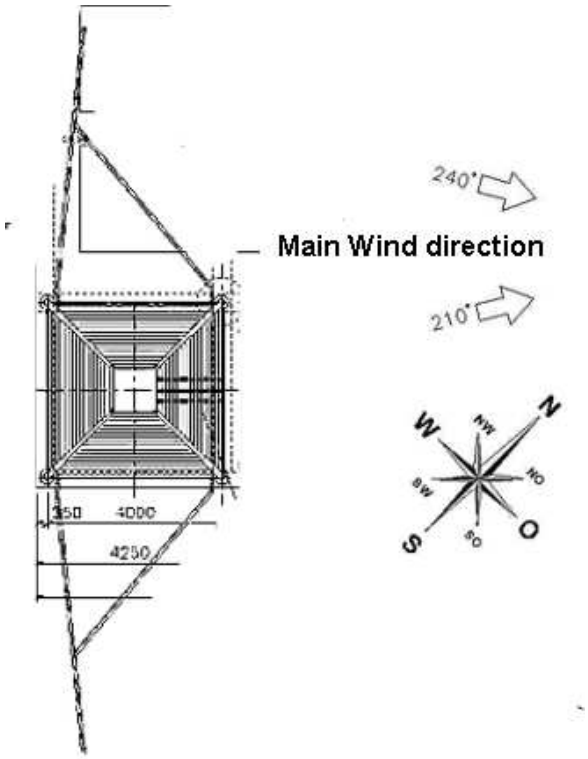

Figure 5.3: Plan view of the measurement platform. Position of cantilevers can be seen well, from Germanischer Lloyd WindEnergie GmbH.

larger relative wind speed than the shadowed sonics. For 310 degrees the wind comes from nearly the opposite direction (it is not exactly 180 degrees, because the two cantilever arms are not exactly 180 degrees opposed, see fig. 5.3), giving the cups the shadow position and consequently the sonics a relatively higher wind speed to measure. Compared with the ground plan of the platform, this behaviour confirms the reliability of the sonic wind speed measurements.

5.2.3 Reliability of the Reference Measurements: Wind Direction

For the two wind vanes at 50 and 70 m height, the data channels used are not intended for direction measurements (personal communication: Tom Neumann 2004). This leads to problems with averaging around zero respectively 360 degrees, which for example leads to an average value of 180 degrees instead of zero if averaged between 355 and 5 degrees. Another problematic behaviour even for angles not close to zero is seen for three of the wind vanes. If differences be-

sonic	installed height at platform
#255	40 m
#273	60 m
#274	80 m

Table 5.1: Installed height of sonics at measurement platform.

tween the measured angles are calculated, one expects to find a constant offset, or a constant behaviour for identical circumstances. But what really is found, are non-distinct shifting angles for the wind direction, shown in fig. 5.6. These shifts are about one to four degrees and do not depend on wind speed, date or wind direction (although the effect only occurs for certain azimuth angles). It is seen that only the wind vane at 30 m shows a consistent behaviour for all configurations. This does also manifest, if wind vane direction measurements are compared to sonic direction measurements.

5.2.4 Quality Control of the Sonic Wind Direction

As we have seen in the previous subsection, only the wind vane at 30 m height can be used as a reference. Comparisons between these data and the sonic data show a constant shift in the sonic measurements. This indicates a misalignment from north direction, which is correctable, if the right offset is known. The shifting angles from north direction for the three sonics are listed in table 5.2. The values are in agreement with those found by the operator of the platform (personal communication: Tom Neumann, 2004).

sonic	Shift from north alignment
#255	54°
#273	277°
#274	29°

Table 5.2: Deviation of the installed sonics from north alignment, value indicates position of true north alignment in sonic coordinate system.

If compared with the reliable wind vane at 30 m, the sonic shows a rather constant shifting angle between 51 and 53 degrees (measurements on the instrument position show a shifting angle of 54 °). The influence of the mast can be clearly seen for wind directions around 125 degrees. For 310 degrees, not enough data was collected to make a reliable statement.

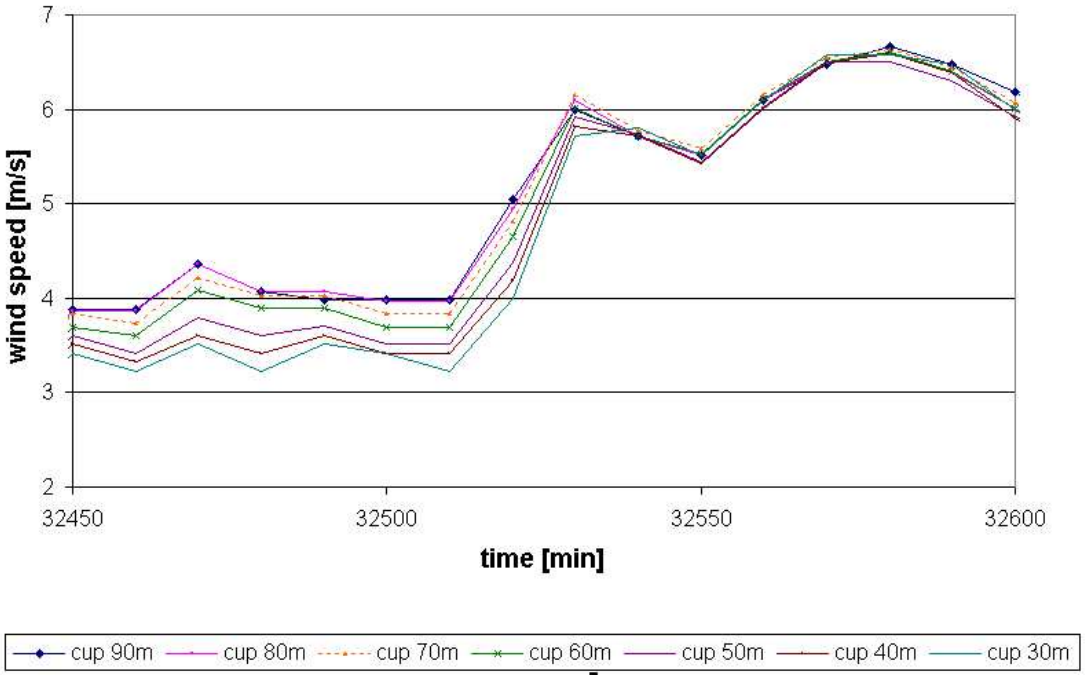

Figure 5.4: Wind speed measured by cup anemometers at different heights over a time span of 2.5 h .

5.2.5 Conclusion

The quality control of the sonics data by comparison with the wind vanes and the cup anemometers show that the installed sonics deliver reliable measurements. Without greater concern, using this data seems justified.
Weaknesses of several measurement instruments, especially the wind vanes, have to be considered.
For the sonics, the shifting angles from north alignment have to be accounted for, additionally wind directions leading to shadowing from the measurement mast have to be treated carefully. If not corrected, these measurements should be taken out of the evaluation, which is done in the following.

5.2.6 Data Selection

In the following, measurement data from November 2003, from the sonics at 40m and 60m height have been used. Following days have been left out, because of missing (m) measurement data or flawed (f) measurements: 10th (mf), 13th (m), 16th (m), 17th (mf), 21st (f), 22nd (f), 27th (mf) and 30th (m) of November.

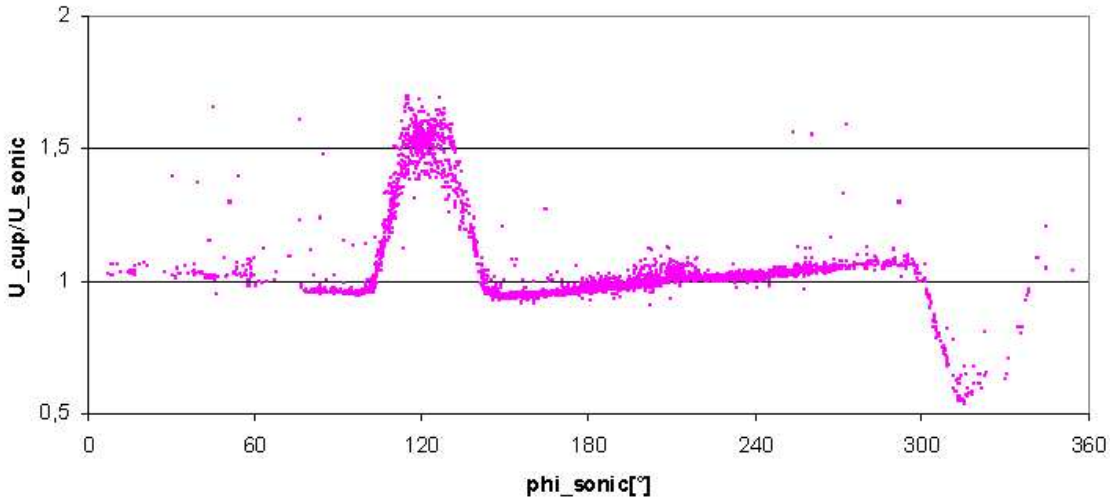

Figure 5.5: Ratio of wind speed measured by cup anemometer and sonic versus wind direction from 0 to 360 degrees. The influence of the measurement mast can easily be seen. Sonic $\#255$, mean value of cup anemometers at 30m and 50m.

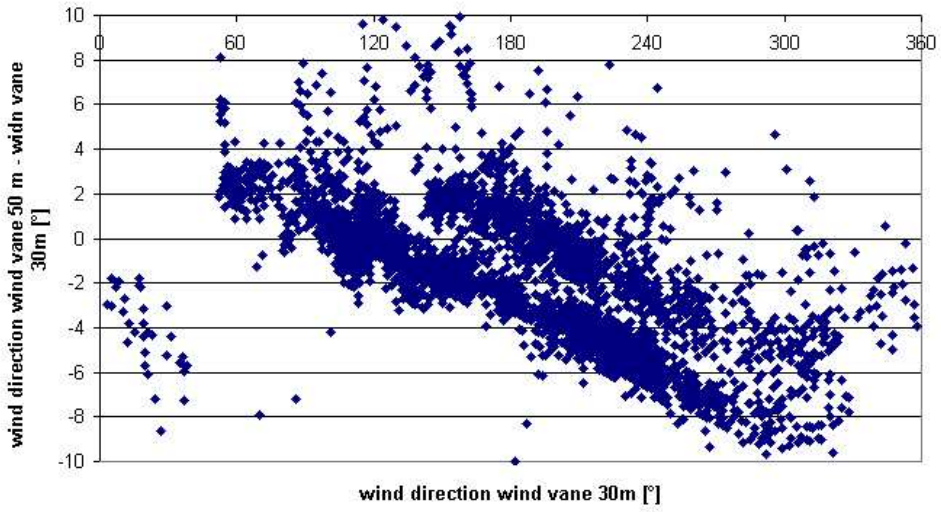

Figure 5.6: Difference of the wind direction measured by the wind vanes at 30m and 50m.

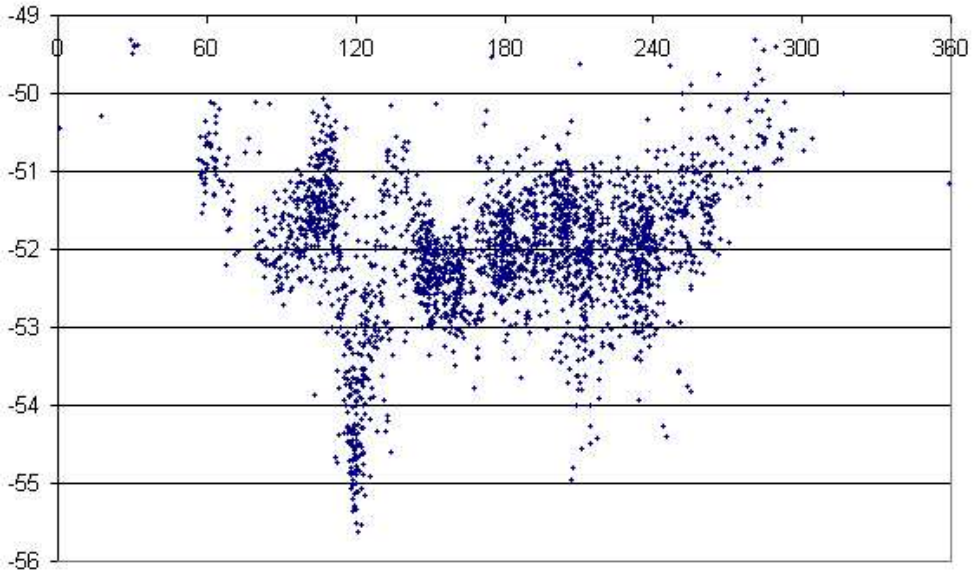

Figure 5.7: Difference of sonic (40m) and wind vane (30m) wind direction measurement versus wind vane (30 m) wind direction measurement.

Chapter 6

Measurement of Heat and Momentum Fluxes in the Surface Layer over the Northern Sea

6.1 Comparison of Corrected and Uncorrected Data

For a first comparison, the monthly mean values from the corrected and the uncorrected measurements are shown in tab. 6.1. The changes for H are similar for both heights, the relatively large magnitude of change for H originating from the influence of the vertical component. Because the applied correction makes the largest relative changes for the vertical component, the large change is not surprising. The changes for u_* are rather similar as well, but for u_* has to be kept in mind that a 10 minutes average of the measurements was used to derive u_*, leading to a quite large sampling error.
U changes differently for each height, adding to the wind speed at 40m and lowering it at 60m. The magnitude of change is the same, the different algebraic signs might origin from slightly different wind directions, which can lead to very different correction values at steep slopes of the lookup table. The change of z/L is different for every height. The large difference could be because of the fact, that the sampling error of u_* grows considerably, when u_* is used in the third power, as for calculation of L.

For the frequency distributions of U, H, u_* and z/L, no significant trend can be found, but the changes are visible, as pictured in fig. 6.1 for friction velocity and sensible heat flux.

If the difference of the uncorrected and corrected values is plotted versus the wind direction, one would expect to find a periodic behaviour for the difference, because the strongest correction applies around the struts. This is confirmed for

40m	corrected	*uncorrected*	change [%]
U	10.242	*10.37054*	-1.24
u_*	0.32826	*0.32991*	-0.5
H	11.60164	*12.3916*	-6.37
z/L	-0.35331	*-0.39429*	-10.39
60m	corrected	*uncorrected*	change [%]
U	10.63507	*10.46695*	1.61
u_*	0.35713	*0.36144*	-1.19
H	12.48541	*13.39198*	-6.77
z/L	-0.50177	*-0.50946*	-1.51

Table 6.1: Monthly mean values of U, u_*,H and z/L for heights of 40m and 60m, derived from corrected and uncorrected measurements, November 2003.

the ratio between the uncorrected and corrected wind speed in fig. 6.2.
To visualize the effect of the changes applied, a plot of the uncorrected and the corrected wind speed is shown in fig. 6.3.

6.2 Overview over Measured Data

A first overview of the data collected is given by tab. 6.1, where the monthly mean values of wind speed, sensible heat flux, friction velocity and z/L are presented for the sonics at 40m and 60m height.
The wind speed at 60m is larger than the wind speed at 40m, thus showing an expected behaviour. For the other quantities, 40m values are always below the 60m ones. This indicates more turbulent movement in the region of 60m. For the friction velocity, this is remarkable, because u_* is a measure of the turbulence of the surface stress, and therefore should decrease with growing height.

6.2.1 Time Series

Wind Speed

The two time series of wind speeds measured by the sonics at 40m and 60m are plotted in fig. 6.4. Both measurements are rather consistent. The wind speed at 60m is predominantly higher than the wind speed at 40m.

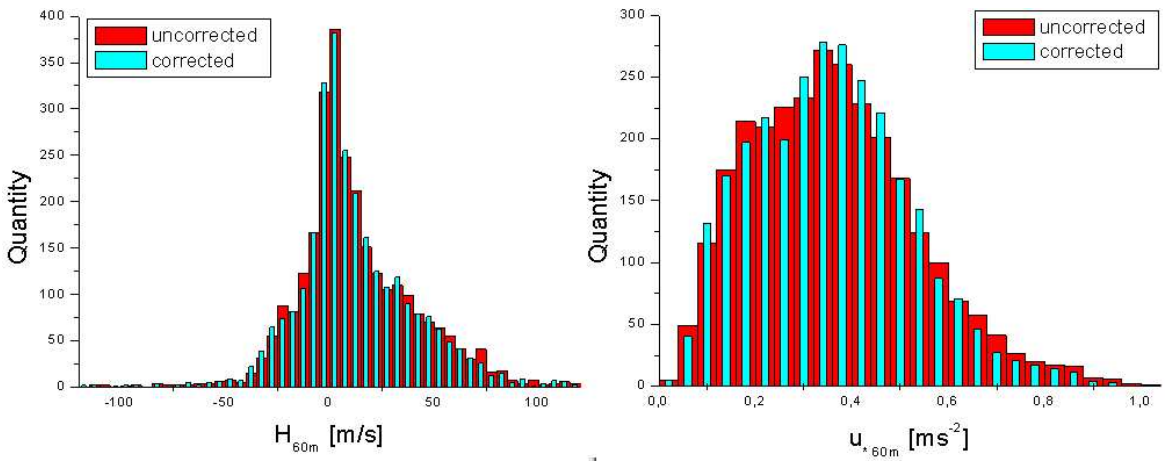

Figure 6.1: Frequency distributions for friction velocity and sensible heat flux at a height of 40m, corrected and uncorrected values, November 2003.

Friction Velocity

Comparing both time series to each other (see fig. 6.11) shows that at a height of 60m generally a higher u_* is measured than at a height of 40m. Especially in week two, the difference is obvious. It would be interesting to examine the closer circumstances of this strong difference, like temperature and wind direction. In weeks one and three, there are some significantly different situations, where the measurement at 40m shows the higher values, these situations are seldom though.

Sensible Heat Flux

The overall course of the sensible heat flux is quite the same for both heights, being higher at 60m than at 40m mostly. For the first two weeks, the heat flux is mostly positive, indicating heat flux from the water to the air. In the third week, the heat flux is mostly negative. And in the last week, positive and negative heat flux are balanced. The scatter found for 60m is much higher than at the height of 40m, as can bee seen in fig. 6.6.

z/L

Plotted versus the time span of the month in fig. 6.7, z/L shows a consistent behaviour. For the first two weeks of the month, unstable stratification dominates. In the end of the third week, stable stratification is found, which occurs more seldom. For the last days, the behaviour is rather mixed, with large scattering.

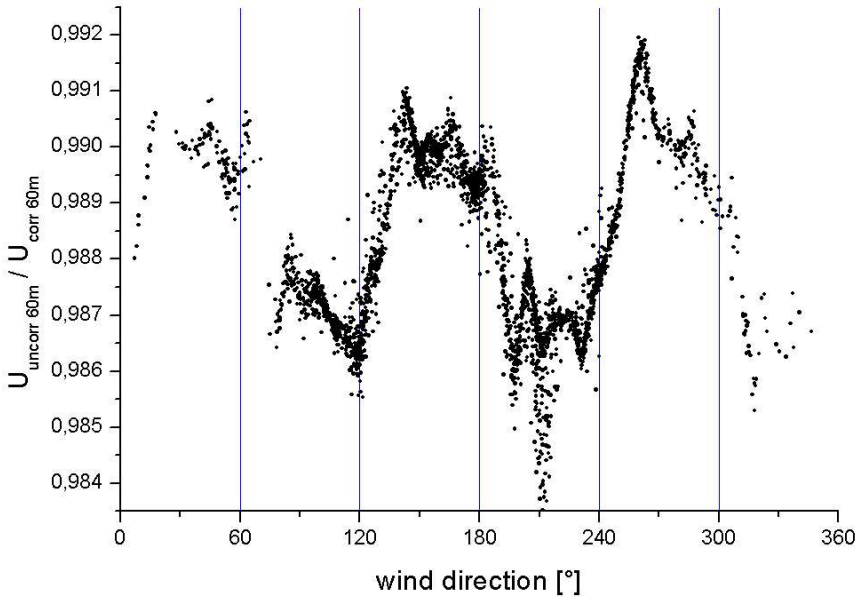

Figure 6.2: Ratio of uncorrected and corrected wind speed plotted versus the uncorrected wind direction, height of 60m, November 2003.

This agrees with the measured sensible heat flux, which is mostly positive for the first two weeks, negative for the third week and mixed for the last week. The connection between these two quantities is described in section 2.1.4.

6.2.2 Frequency Distribution

The frequency distributions for U, u_*, H and z/L show the characteristics found in the already presented time lines and monthly means more clearly. For friction velocity and z/L the algebraic signs are most interesting, because they characterize different atmospheric behaviour. Therefore frequency distributions of these two are shown.

Sensible Heat Flux

The frequency distribution of both heights shows the dominance of positive values for H, similar for both heights, see fig.6.8. This indicates a domination of heat rising from the water in the air. This agrees with the mostly unstable atmospheric stability found.

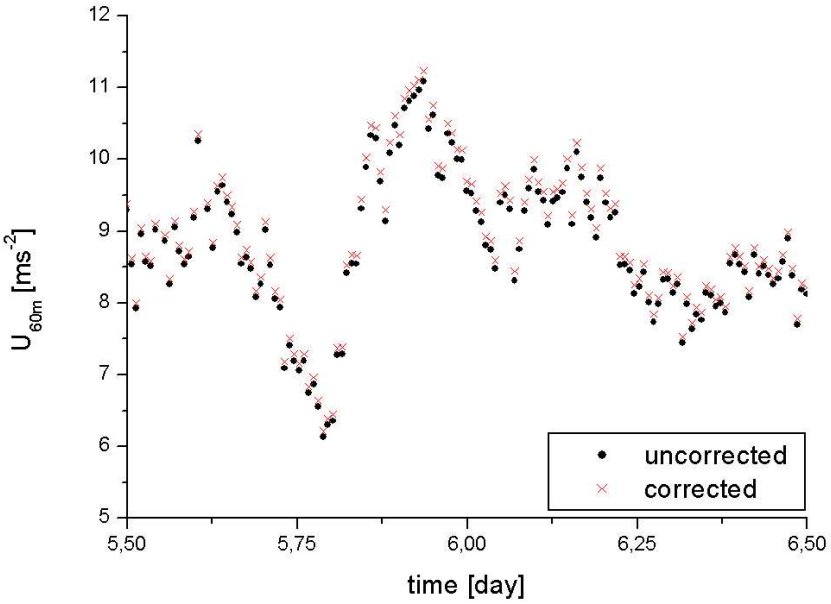

Figure 6.3: Uncorrected and corrected wind speed plotted versus time, height of 60m, November 2003.

$\mathbf{z/L}$

As was seen at the time series, negative values of z/L dominate, although some positive values are found as well. This is identical for both heights. Here the mostly unstable stratification of the atmosphere for both heights is shown, see fig. 6.9.

6.3 Comparison of Measurements at Different Heights

In the previous sections, already the different heights were compared to each other. In this section the daily variations for the heights are compared to give a better understanding of the daily processes. Two quantities bearing a recognizable diurnal cycle are presented. Additionally, the measurements at the two heights are directly compared to each other. This allows to recognize linear or other coherences easily.

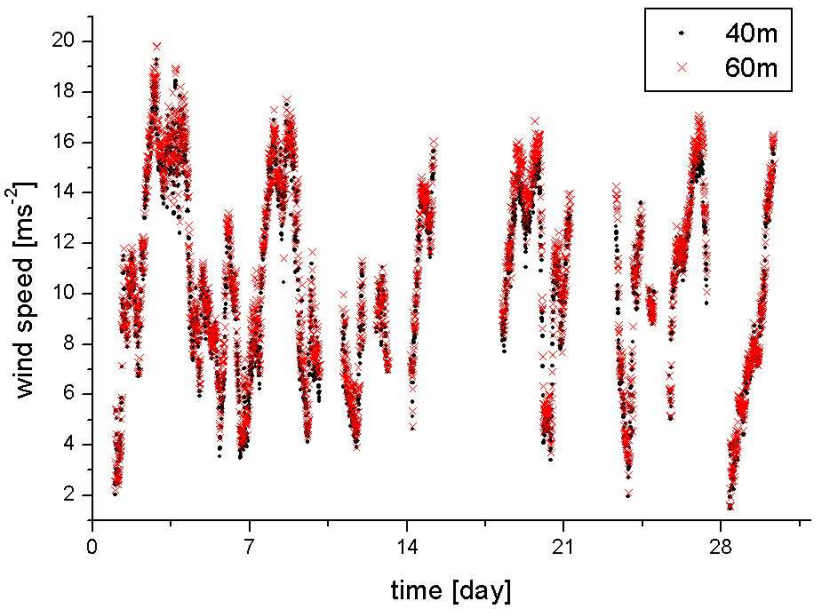

Figure 6.4: 10 min averages of wind speed at 40m and 60m versus the time span of the month, November 2003.

6.3.1 Diurnal Variation

Wind Speed

Mean values for each hour of the day are shown in fig. 6.10. For both heights, wind speed rises over the course of the day having its lowest point at approx. 3h in the morning.

Friction Velocity

Over the course of the day, u_* behaves similar at the heights of 40m and 60m. It is characterized by two minima slightly after 3h and around 12h and two maxima around 8h and 19h. The friction velocity at 60m is higher than the one at 40m, as can be seen in in fig. 6.11.

6.3.2 Direct Comparison of Both heights

Wind Speed

If U_{60m} is plotted versus U_{40m}, as in fig. 6.12, it can be seen that the general trend is linear. It shows again, that at 60m height, the wind speed is constantly higher

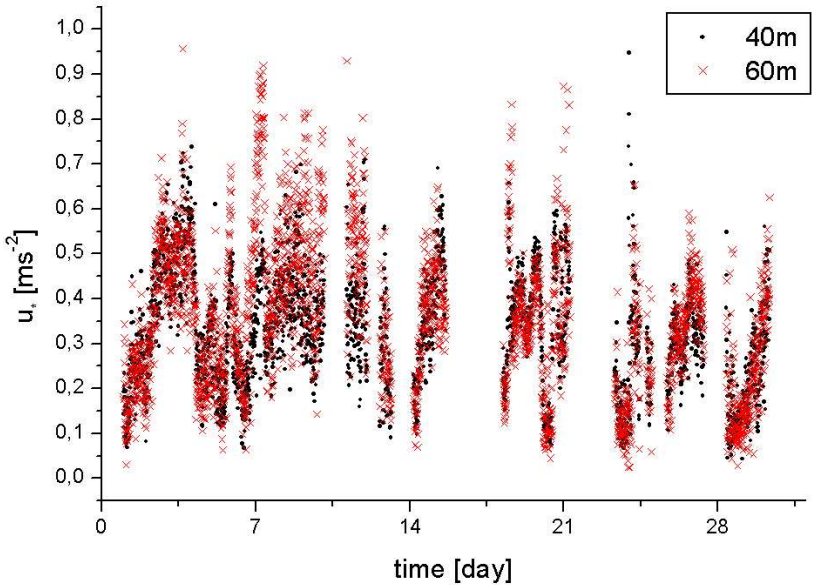

Figure 6.5: u_{*60m} and u_{*40m} versus the time span of the month, November 2003

as at 40m, as the region above the bisecting line is much more populated.

Friction Velocity

A tight cone shape is found if both friction velocities are plotted against each other (fig. 6.13). The variance of both rises with rising friction velocity. More higher values are found for the height of 60m.

Sensible Heat Flux

If plotted against each other (fig. 6.14), a scattered cloud can be seen, which shows a linear behaviour for positive values of H and for negative values H_{60m} has a smaller magnitude than H_{40m}, resulting in a nearly parable form. The behaviour has to be examined further for the negative values, because not enough measurements where found with negative values of H.

z/L

The two z/L compared show for both positive or both negative values strong scattering, shown in fig. 6.15. Values where $60/L$ and $40/L$ differ in algebraic signs are more seldom and mostly close to the origin. The scattering is strong,

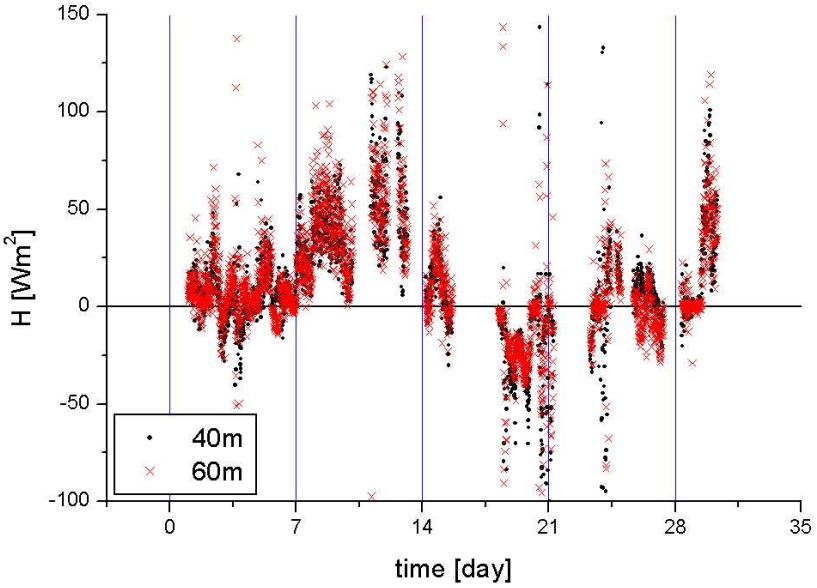

Figure 6.6: H_{60m} and H_{40m} versus each day of the month, November 2003

because of the large scattering in L itself, being derived from the 3rd power of the friction velocity. The friction velocity has a large sample error, which is amplified by the third power.

6.4 Conclusion

- For the influence of the correction method, the correction changes become especially apparent for the heat flux, mainly because of the initial correction of the important vertical component. For the other quantities, the change because of correction is clearly visible as well.
- A longer averaging time would reduce the sampling error of u_*. A less scattered L could result from such a change.
- The measurements are found to be consistent. Changes in the atmospheric stability are confirmed by accordant changes in heat flux for example.
- After viewing the measurements, it seems that at a height of 60m the atmosphere is more turbulent than at 40m height. This is evidenced by the higher friction velocity and quite unusual. Further investigation should be

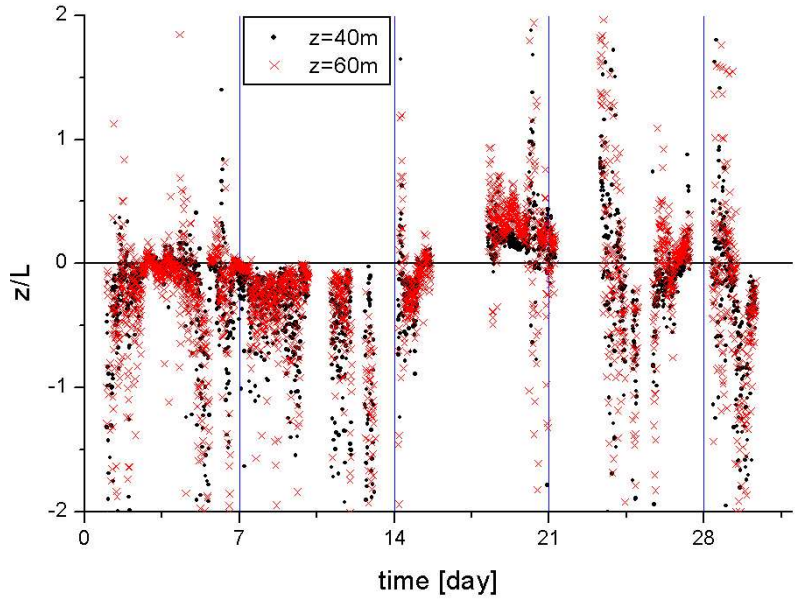

Figure 6.7: z/L for heights of 40m and 60m versus the time span of the month, November 2003

conducted. Adding of the measurements at 80m height could prove interesting.

6.5 Outlook

After a correction for the employed sonics was developed and the validity of the measurement data is confirmed, further investigation of the atmosphere over the north sea should be conducted.

- Until now, only measurements from the sonics at 40m and 60m height have been used. Adding the third sonic at 80m height would complete the profiles for wind speed, friction velocity, heat flux and z/L. Especially the friction velocity at 80m would be of interest.
- Adding more measurement data from different month would make it possible to look for seasonal variation, especially for the diurnal circles and the atmospheric stabilities.

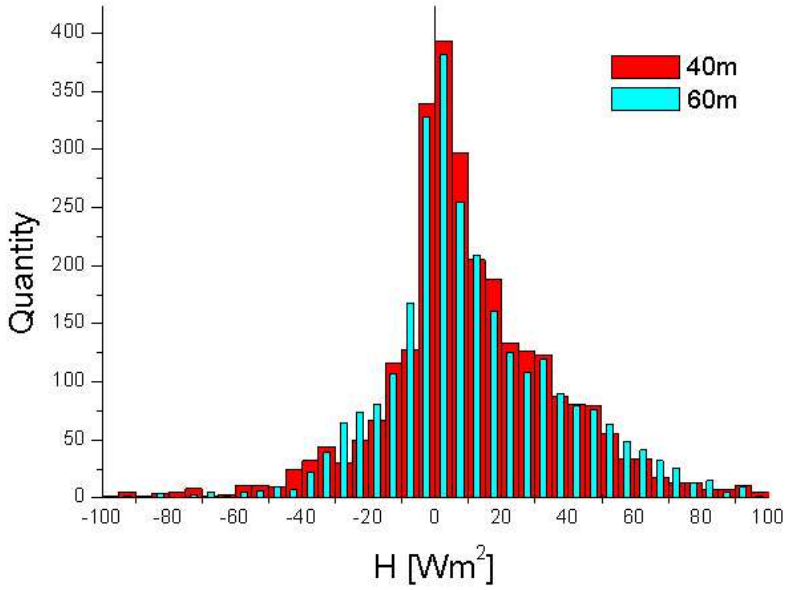

Figure 6.8: Frequency Distributions of H_{60m} and H_{40m}, November 2003.

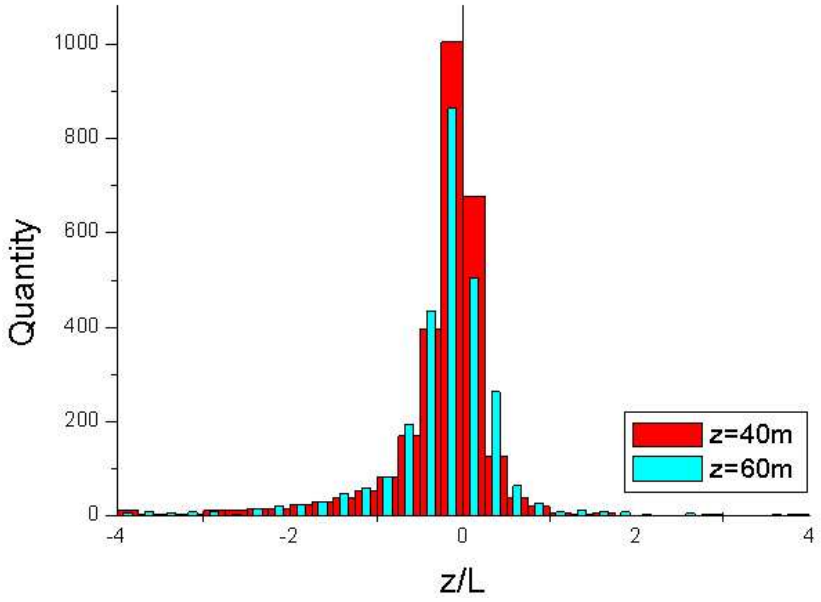

Figure 6.9: Frequency distributions of z/L for heights of 40m and 60m, November 2003.

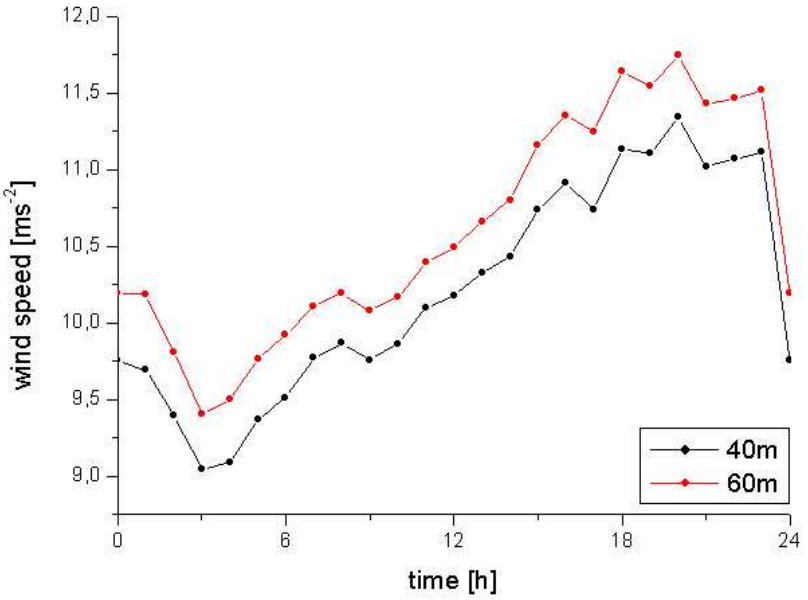

Figure 6.10: Mean wind speed values of both heights versus the time span of the day, November 2003.

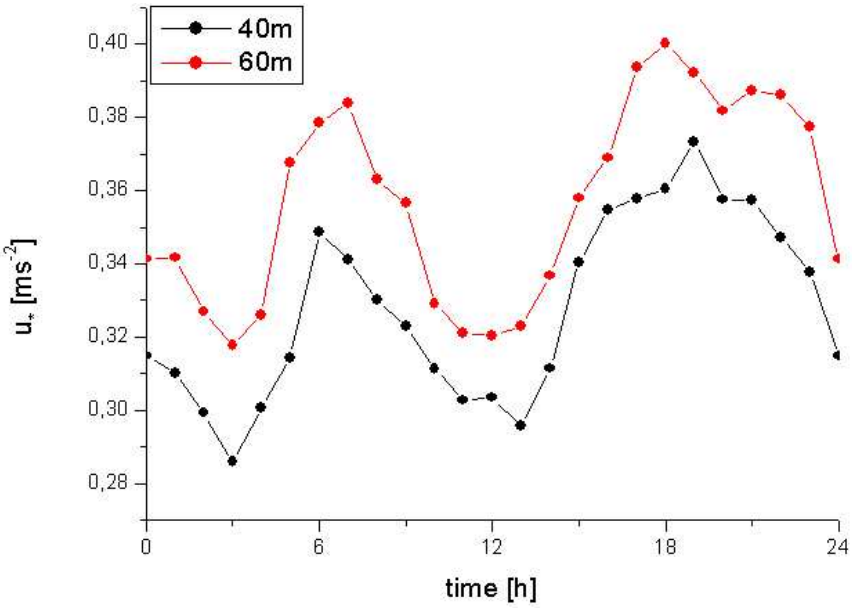

Figure 6.11: $u_{*60m\ mean}$ and $u_{*40m\ mean}$ versus the time span of the month, November 2003.

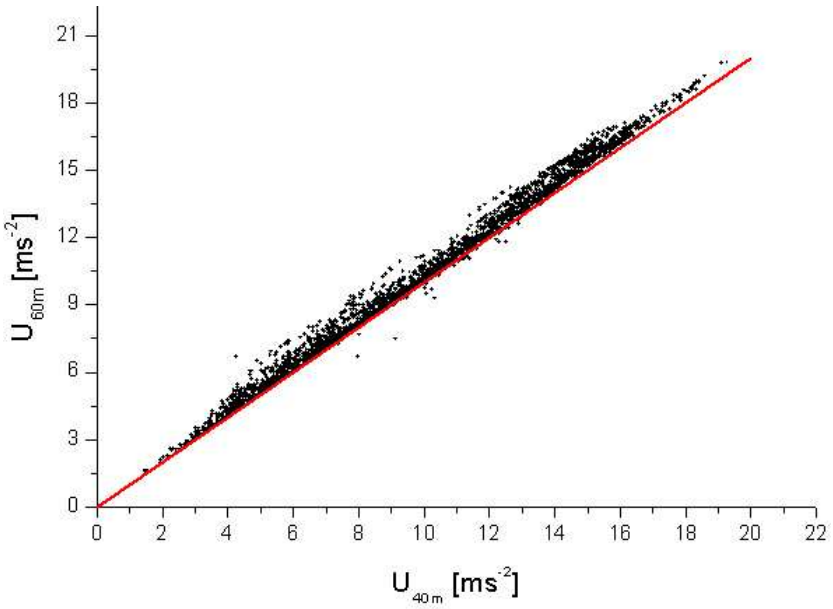

Figure 6.12: U_{60m} versus U_{40m} and the bisecting line, November 2003.

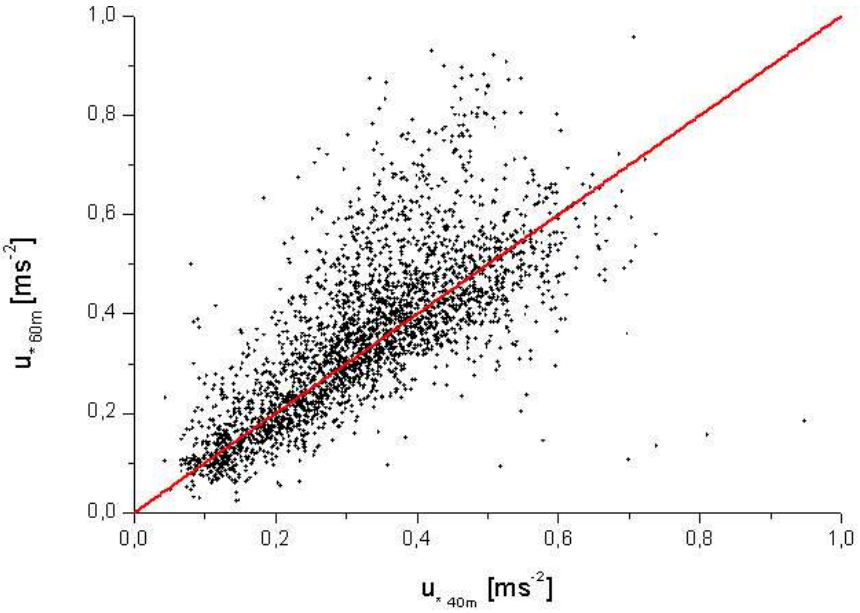

Figure 6.13: u_{*60m} versus u_{*40m} and the bisecting line, November 2003.

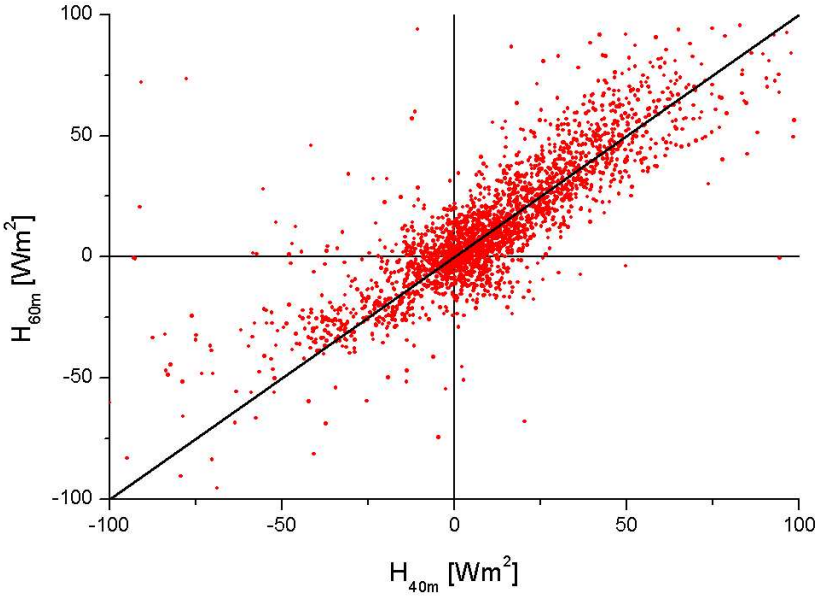

Figure 6.14: H_{60m} versus H_{40m} and the bisecting line, November 2003.

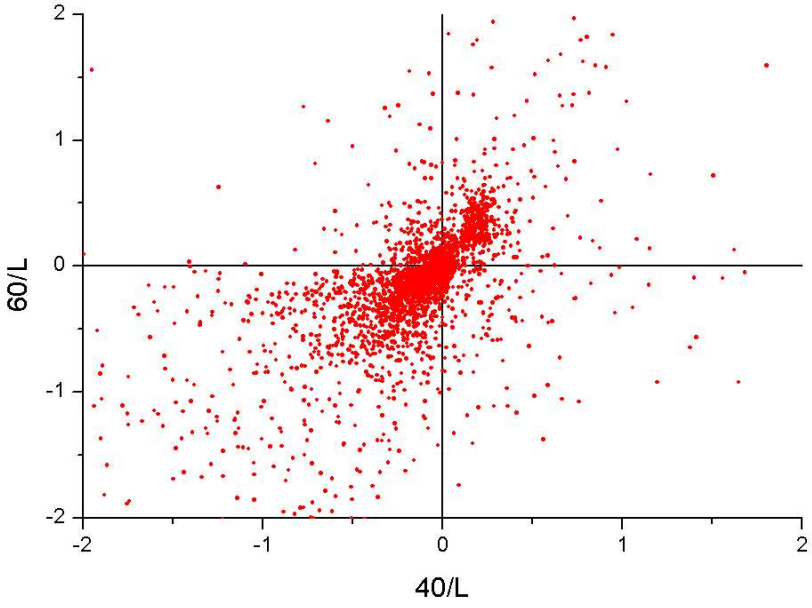

Figure 6.15: $60/L$ versus $40/L$, November 2003.

Chapter 7

Conclusions

Three ultrasonic anemometers (Gill Instruments Ltd., model 1210R3-50) are employed at the offshore measurement platform FINO I, which is positioned 45 km north of Borkum in the North Sea.
Prior to installation, the calibration of the three ultrasonic anemometers was tested in the Oldenburg wind tunnel. Flaws in the calibration were found and therefore an empirical correction method for the calibration was developed and applied. The correction of the calibration was tested successfully.
After ensuring the validity of the measurement data from FINO, an initial analysis of field data was performed. Flux measurements were derived for one month and first investigations of the atmospheric stability and diurnal cycles were conducted.

The factory-installed calibration of the sonic anemometers was tested in the Oldenburg wind tunnel. Systematic errors similar at all three sonics as well as errors which are specific for each individual instrument were found in wind tunnel measurements. Around the struts, the measured wind speed can deviate up to 3 % from the reference wind speed. Additionally, the uncorrected vertical component proves to be problematic, erroneous vertical wind speeds of up to 0.1 m/s for a reference speed around 10 m/s were found. If the measurements should be used for flux calculations, an enhancement of the calibration is needed. This applies not only for the instruments used, but shows that the factory-installed calibration for the sonics should be treated with caution if used for flux measurements.

A correction method for the calibration of the sonics has been developed, based on the measurements . The correction is azimuth and elevation angle dependent and makes use of symmetries and linearities found in the behaviour of the sonic in the flow. Therefore the correction employs a limited number of wind tunnel measurements, making is usable even if only short time is available for testing the sonic. The improvements could be shown, especially for the vertical

component.

A quality control of the measurements made by the FINO measurement platform was conducted, to ensure valid data. The measurements made by cup anemometers and sonics showed to be consistent, while for three of the four wind vanes different problems occurred. Two of the wind vanes are not connected to a channel designed for direction measurements, three of the wind vanes show a non distinct shifting angle from north alignment.
The shifting angles from north alignment for the three sonics could be determined and validated with data from the operator of the platform. Additionally, wind directions leading to mast shadowing could be determined.

For one month fluxes were calculated from the corrected measurement data. They show a mostly unstable stratification for November 2003. While the wind profile seems to behave as expected, the friction velocity rises with increasing height, which is unexpected. This effect has to be investigated further. Diurnal variations for wind speed and friction velocity could be found, showing a diurnal cycle with strong minima and maxima. The effect of the corrected calibration was showed as well.
However only one month of data was used in this initial analysis. To verify these findings, a longer time period has to be considered.

Bibliography

[1] J.A. Businger, J.C. Wyngaard, Y. Isumi, E.F. Bradley: *Flux-profile relationships in the atmospheric surfaec layer.*, Journal of Atmospheric Science, Vol. 28, pp 181-189, 1971

[2] Institute for Technical and Applied Physics (ITAP): *Strömungsakustische Messungen im Windkanal*, Internal Report, University of Oldenburg

[3] Deutscher Kalibrierungsdienst: *Leitfaden für Volumenbestimmung bei Referenzmessproben in medizinschen Refrenzlaboratorien*, Teil 1, 2002

[4] T. Foken: *50 Years of the Monin-Obukhov Similarity Theory*, Extended Abstract, 16th Symposium on Boundary Layers and Turbulence, Portland, 2004

[5] J.H.C. Gash, A. J. Dolman: *Sonic anemometer (co)sine response and flux measurement I. The potential for (co)sine error to affect sonic anemometer-based flux measurements*, Agricultural and Forest Meteorology, Vol. 119, pp 195-207, 2003

[6] Gill Instruments Limited: *"R3-50 Ultrasonic Research Anemometer"*, Datasheet, 2001

[7] A. Grelle, A. Lindroth: *Flow Distortion by a Solent Sonic Anemometer: Wind Tunnel Calibration and its Assessment for Flux Measurements over Forest and Field*, Journal of Atmospheric and Oceanic Technology, Vol. 11, pp1529-1542, 1994

[8] U. Högström, A.S. Smedman: *Accuracy of sonic anemometers: Laminar wind-tunnel calibrations compared to atmospheric in situ calibrations against a reference instrument*, Boundary Layer Meteorology, Vol. 111, pp 33-54, 2004

[9] J. C. Kaimal, J. J. Finnigan: *Atmospheric Boundary Layer Flows*, Oxford University Press, New York, 1994

[10] M.K. van der Molen, J.H.C. Gash, J. A. Elbers: *Sonic anemometer (co)sine response and flux measurement II. The effect of introducing an angle of attack depentent calibration.*, Agricultural and Forest Meteorology, Vol. 122, pp 95-109, 2004

[11] Tom Neumann, Deutsche Windenergie-Institut GmbH: *personal communication*, 2004

[12] M.W. Rotach: *Turbulence within and above an urban canopy*, PhD Thesis, Zürich, 1991

[13] U. Stabe, D. Langner: *Messung und Simulation systematischer Fehler des Ultraschallanemometers und deren Auswirkungen auf statistische Größen*, Diploma Thesis, Oldenburg, 1997

[14] R. B. Stull: *An Introduction to Boundary Layer Meteorology*, Kluwer Academic Publishers, Netherland, 1988

[15] D. Westermann, Deutsche WindGuard GmbH: *personal communication*, 2003

[16] J.M. Wilczak, S.P. Onceley, S.A. Stage: *Sonic Anemometer Tilt Correction Algorithms*, Boundary Layer Meteorology, Vol 99., pp 127-150, 2000

[17] A. Wiesner, F. Fiedler, U. Corsmeier: *The Influence of the Sensor Design on Wind Measurements with Sonic Anemometer Systems*, Journal of Atmospheric and Oceanic Technology, Vol. 18, pp 1585-1608, 2001

[18] J.C. Wyngaard: *The Effects of Probe-Induced Flow Distortion on Atmospheric Turbulence Measurements*, Journal of Applied Meteorology, Vol. 20, pp. 784-794, 1981

[19] J.C. Wyngaard, S.F. Zhang: *Transducer-shadow effects on turbulence spectra measured by sonic anemometers*, Journal of Atmospheric and Oceanic Technology, Vol.2, pp 548-558, 1985